Dissertation for the Doctoral Degree

Studies of the Functions of Tumoricidal Factors on MS-K Tumor Formation and Angiogenesis

Name: XING Yanjiang

Doctoral Program in Life and Food Science

Graduate School of Science and Technology

Niigata University

Contents

Abbreviation 5

Abstract 6

概要 9

1. Introduction 12

1.1 Tumor microenvironment 12

1.2 Granulocytes in tumors 13

1.3 The differences between MS-K and NFSA tumor cells 14

1.4 Overview of this research 17

2. Materials and Methods 18

2.1 Mice 18

2.2 Cells 18

2.3 Construction of pIRES2-IL-18-ZsGreen1 and pIRES2-CCL11-ZsGreen1 18

2.4 Establishment of MS-K-IL-18 and MS-K-CCL11 19

2.5 Analysis of gene expression by RT-PCR and qPCR 19

2.6 Cell proliferation assay 20

2.7 Colony formation assay 20

2.8 Confocal microscope observation of MS-K overexpressing clones 20

2.9 Quantification of IL-18 and CCL11 in the CM of overexpressing clones 21

2.10 Tumor formation assay 21

2.11 immune cells infiltration analysis in the tumors 21

2.12 Differentiation of eosinophils by CCL11-stimulation 23

2.13 Transwell migration assay 23

2.14 Co-culture of induced eosinophils and tumor or endothelial cells 24

2.15 CCR3 antagonist injection into NFSA tumor-bearing mice 24

2.16 Immunohistochemical staining of paraffin-embedded tumor sections 24

2.17 Statistical analysis 25

3. Results 26

3.1 The function of IL-18 on MS-K tumor formation and angiogenesis 26

3.1.1 The establishment of IL-18 overexpressing MS-K clones 26

3.1.2 The protein expression in the MS-K-IL-18 clones 28

3.1.3 The characterization of MS-K-IL-18 clones *in vitro* 29

3.1.4 The effect of IL-18 on tumor formation and angiogenesis 31

3.1.5 The effect of IL-18 on immune cells infiltration and polarization 34

3.1.6 The effect of IL-18 stimulated macrophage on endothelial cells 35

3.1.7 Summary 36

3.2 The function of CCL11 on tumor formation and angiogenesis 38

3.2.1 The establishment of CCL11 overexpressing MS-K clones 38

3.2.2 The protein expression in the MS-K-CCL11 clones 40

3.2.3 The characterization of MS-K-CCL11 clones *in vitro* 42

3.2.4 The effect of CCL11 on granulocyte differentiation 43

3.2.5 The effect of CCL11 on granulocyte migration 46

3.2.6 The eosinophil infiltration in the NFSA tumors 48

3.2.7 The effect of the CCL11 induced-eosinophils on tumor and endothelial cells 49

3.2.8 The effect of specific CCR3 antagonist on NFSA tumor 51

3.2.9 Summary 54

4. Discussion 56

4.1 Characteristics of IL-18-overexpressing MS-K 56

4.2 Effect of IL-18 on polarization M1 macrophages in the MS-K-IL-18 tumor 56

4.3 IL-18-stimulated macrophages caused apoptosis in endothelial cells 57

4.4 Pro-inflammatory genes in the CD14+Gr-1+ cells 58

4.5 Effect of CCL11 on growth of the tumor 59

4.6 Effect of CCL11 on differentiation of the granulocyte 59

4.7 Effect of CCL11 on recruitment of the eosinophil 60

4.8 Effect of CCR3 antagonist on NFSA tumor growth 61

4.9 Conclusion 61

Reference..... 62

Supplemental Table1. List of PCR primers 71

Supplemental table 2. Comparisons of Xbp1 expression in MS-K and NFSA cells 73

Acknowledgements..... 74

Abbreviation

Abbr.	Full Name	Abbr.	Full Name
IL-18	Interleukin-18	CD14	cluster of differentiation 14
CCL11	C-C chemokine ligand 11	CM	Conditioned Medium
CCR3	C-C chemokine receptor	BSA	Bovine serum albumin
VEGF	Vascular endothelial growth factor	PDGF	Platelet-derived growth factor
M-CSF	Macrophage-colony stimulating factor	G-CSF	Granulocyte-colony stimulating factor
PI	Propidium iodide	DAB	3,3'-Diaminobenzidine
ANG	Angiopoietins	FGF	Fibroblast growth factor
HGF	Hepatocyte growth factor	DAPI	4',6-diamidino-2-phenylindole
IFN-γ	Interferon-gamma	Gr-1	Ly-6G/Ly-6C
TGF-β	Transforming growth factor-beta	TNF-α	Tumor necrosis factor alpha
Siglec-F	Sialic acid-binding immunoglobulin-like lectin F	Cela2a	Chymotrypsin like elastase family member 2A
MMP-9	Matrix metallopeptidase 9	Egln1	Egl nine homolog 1
TATEs	Tumor-associated tissue eosinophils	Mrc1	Mannose Receptor, C Type 1
DCs	Dendritic cells	Nos2	Nitric oxide synthase 2
α-MEM	Minimum Essential Medium Eagle (MEM). Alpha Modifications	DMEM	Dulbecco's Modified Eagle's Medium

Abstract

Tumor growth depends on angiogenesis, which transports the oxygen and nutrients to the tumor cells and provides an essential microenvironment for the tumor growth and even metastasis. The tumor-associated angiogenesis, together with the tumor cells, stromal cells and some immune cells, forms the tumor niche. In the tumor niche, various protein factors, such as vascular endothelial growth factors (VEGFs), platelet-derived growth factors (PDGFs), fibroblast growth factors (FGFs), interleukins and chemokines, transduce the signals via their receptors and influence the tumor-associated angiogenesis. A lot of reports demonstrated that the immune cells, resident in the tumor niche, and the protein factors related for the tumor formation and angiogenesis. Nevertheless, the precise anti-tumoral functions of the immune cells remain to be explored further.

Our group previously demonstrated that Interleukin-18 (IL-18) and C-C type chemokine ligand, CCL11 were highly expressed in a NFSA tumor cell line than the MS-K tumor cell line. The NFSA tumor showed limited angiogenesis and severe necrosis. On the other hand, the MS-K tumor showed enriched well-developed blood vessel network. It was thought that IL-18 produced by NFSA cells induced the M1 type of macrophages in NFSA tumors, and it may have resulted in the severe necrosis of NFSA tumors by enhancing macrophage phagocytosis and cytotoxicity. Really, the activated macrophages caused the destruction of endothelial cells *in vitro.* However, the effect of IL-18 on blood vessel formation *in vivo* and the origin of the infiltrated immune cells, into tumor have not been elucidated. Therefore, in this study, I aimed to elucidate the roles of the IL-18 and CCL11 on angiogenesis and accumulation of the immune cells in tumor, using these cell lines.

Firstly, I established IL-18-overexpressing MS-K cell clones (MS-K-IL-18) to address the roles of IL-18 in angiogenesis. The overexpression of IL-18 in MS-K cells inhibited the proliferation rate of the MS-K-IL-18 cells *in vitro* and blood vessel

formation in the MS-K-IL-18 tumors. Interestingly, CD14-positive cells from the MS-K-IL-18 tumor had upregulated expression of the M1 type macrophage marker *il-6*. Furthermore, FACS analysis revealed more accumulation of CD11b+CD80+ M1 macrophages in the MS-K-IL-18 tumors than in the parental MS-K tumor. Moreover, an *in vitro* co-culture assay demonstrated that MS-K-IL-18-conditioned medium (CM) stimulated macrophages to induce the apoptosis of endothelial cells. However, there was no significant difference in the number of the accumulated immune cells in the tumor between the parental MS-K-tumor and MS-K-IL-18-tumor. Thus, it revealed that the IL-18 was not responsible for the immune cell accumulation in the NFSA cells.

Next, I attempted to clarify the relevance of CCL11-recruited immune cells in angiogenesis and tumor formation. Then I established CCL11-overexpressing MS-K cell clones (MS-K-CCL11) to clarify the role of CCL11 on immune cell accumulation and angiogenesis. The proliferation rate and colony formation ability *in vitro* were almost the same between MS-K-CCL11 and parental MS-K cells. However, interestingly, the MS-K-CCL11 cells could not form any tumors in mice. The MS-K-CCL11-conditioned medium and recombinant CCL11 induced macrophage and eosinophil differentiation from bone marrow cells. The MS-K-CCL11-CM effectively attracted eosinophils, which were differentiated from bone marrow cells by the MS-K-CCL11-CM. Furthermore, the eosinophils damaged the MS-K, NFSA and endothelial cells in a dose dependent manner by co-culture experiment. Administration of CCL11-receptor CCR3 specific antagonist SB 328437 into NFSA cells-transplanted mice restored the blood vessel formation and blockaded of eosinophils infiltration into NFSA tumor. These data indicated that the CCL11 was responsible for differentiation of eosinophils, and also recruitment of them into tumor.

Cumulatively, these data demonstrated that IL-18 and CCL11 both have tumoricidal effects on MS-K tumors: Excess IL-18 produced by MS-K-IL-18 induced M1 macrophages and inhibited blood vessel formation by pro-apoptotic capability

exerted by macrophages to endothelial cells. Whereas, excess CCL11 produced by MS-K-CCL11 cells induced and recruited eosinophils to tumor; which would damage not only the MS-K-CCL11 cells but also the endothelial cells and would block MS-K tumor formation. These results indicate that CCL11 and IL-18 are the key factors to modulate the tumor immune cells infiltration and angiogenesis; and also indicates that they would be potential targets of tumor treatment strategy.

概要

腫瘍の成長は血管新生に依存します。その新生血管は腫瘍細胞に酸素と栄養分を輸送して，腫瘍の成長のみならず転移にさえも十分な微小環境をつくり出します。 腫瘍関連の血管新生では，腫瘍細胞，間質細胞および若干の免疫細胞と共に，腫瘍ニッチを形成します。 腫瘍ニッチでは，各種のタンパク質因子，例えば，血管内皮細胞増殖因子（VEGFs），血小板由来増殖因子（PDGFs），線維芽細胞増殖因子（FGFs），インターロイキンとケモカイン等が，それらのレセプターを通して信号を変換して，腫瘍関連の血管新生に影響します。 数多くのレポートが，腫瘍ニッチ内の免疫細胞とタンパク質因子が腫瘍形成と血管新生に関連していることを示しています。 それでも，免疫細胞の抗腫瘍機能は，まだ詳しく調査されないまま残っています。

我々のグループは，以前，インターロイキン-18 (IL-18)と C-C 型のケモカインリガンド 11 (CCL11)が，MS-K 腫瘍細胞に比べて NFSA 腫瘍細胞株で高く発現している事を示しました。NFSA 腫瘍は，限定的な血管新生と重篤な壊死という特徴を示します。一方，MS-K 腫瘍は，豊富な良く発達した血管ネットワークを持ちます。NFSA 細胞によって産生された IL-18 は，NFSA 腫瘍中で M1 タイプのマクロファージを誘導して，これがマクロファージの貪食能と細胞傷害性を増強することによって NFSA 腫瘍の壊死を引き起こしているものと考えられます。実際に活性化されたマクロファージは，試験管内で内皮細胞の破壊を引き起こします。しかしながら，IL-18 の生体内における血管新生に対する役割，および肉腫に浸入する免疫細胞の起源は，解明されていませんでした。そこで私はこれらの細胞系を使用して，腫瘍に於ける血管新生と免疫細胞の蓄積に対する IL-18 と CCL11 の役割を解明しようとしました。

まず始めに私は IL-18 の血管新生に及ぼす役割を明らかにするために，IL-18 を過剰発現する MS-K 細胞クローン株（MS-K-IL-18）を樹立しました。 IL-18 の過剰発現は，インビトロにおいて MS-K-IL-18 細胞の増殖率， および MS-K-IL-18 腫瘍にお

ける血管新生を抑制しました。興味深いことに，MS-K-IL-18 腫瘍由来の CD14 陽性の細胞は，M1 タイプマクロファージのマーカーであるインターロイキン 6 の発現を上昇させました。さらにその上，FACS 解析は，親株の MS-K 腫瘍より MS-K-IL-18 腫瘍において CD11b+CD80+ M1 マクロファージのより多くの蓄積を明らかにしました。さらに，MS-K-IL-18 の調製培地で刺激されたマクロファージは，血管内皮細胞のアポトーシスを誘導する事がインビトロの共培養分析により明らかにされました。しかしながら，肉腫に集まった免疫細胞数に関しては，親株である MS-K-腫瘍と MS-K-IL-18-腫瘍の間に有意差はありませんでした。従って，IL-18 は NFSA 肉腫に於ける免疫細胞の蓄積には無関係である事が示されました。

次に私は CCL11 に動員された免疫細胞の血管新生と腫瘍形成における役割を明らかにしようと試みました。そこで，免疫細胞蓄積と血管新生に関して CCL11 の役割を明確にするために，CCL11 を過剰発現する MS-K細胞クローン（MS-K-CCL11）を樹立しました。試験管内における増殖率とコロニー形成能力は，MS-K-CCL11 と親株の MS-K細胞の間で殆ど同じでした。しかし，興味深いことに，MS-K-CCL11 細胞は, マウスで腫瘍を形成することができませんでした。MS-K-CCL11 の調製培地（CM）および組み換え型 CCL11 は，骨髄細胞からマクロファージと好酸球分化を誘導しました。また，MS-K-CCL11-CM を用いて骨髄細胞から好酸球を分化誘導させ MS-K-CCL11-CM の誘引能を調べると，効果的に好酸球を引きよせました。さらにまた，好酸球はインビトロの共培養実験により細胞数依存的に MS-K 細胞，NFSA 細胞そして内皮細胞に傷害を与えました。そして CCL11-レセプターである CCR3 に対する特異的阻害薬 SB 328437 を NFSA 細胞が移植されたマウスへ同時投与すると，肉腫中の一部の血管新生が回復し，NFSA 腫瘍への好酸球の浸入が遮断されました。これらのデータは，CCL11 が好酸球の分化，更には腫瘍への好酸球の誘引を行うことを示しました。

まとめると，以上のデータは IL-18 と CCL11 が MS-K 腫瘍に両方とも殺腫瘍効果を持つことを証明しました。MS-K-IL-18 によって産生される過剰な IL-18 は，M1 タイプマクロファージを誘導して，内皮細胞にアポトーシスを誘導する事によってこれを傷害し，血管新生を妨げました。一方，MS-K-CCL11 細胞によって産生される過剰な CCL11 は，好酸球を分化誘導して，この細胞を肉腫へ誘引しました。そして，誘引された好酸球は内皮細胞のみならず MS-K-CCL11 細胞にも傷害を与えて，MS-K 腫瘍形成を妨げました。これらの結果は，CCL11 と IL-18 が腫瘍への免疫細胞浸入と血管新生を調整する鍵となる要因であることを示します。そしてこれらが腫瘍治療戦略の潜在的標的であることを示します。

1. Introduction

1.1 Tumor microenvironment

Tumorigenesis is modulated by abnormal immune responses and upset homeostasis [1]. The environment in the tumor has diverse capacities to induce both positive and negative effects for tumorigenesis. Therefore, the cells or factors in the tumor environment were educated into various functions in the tumor niche.

It has been postulated that tumorigenesis is associated with the formation of new blood vessels, namely angiogenesis [2]. To date, studies on angiogenesis are explosively increasing, following by more soluble pro-angiogenic factors determined as therapeutic targets. The most notable one was vascular endothelial growth factors (VEGFs) and their receptors [3-5]. Beyond the VEGF/VEGFR pathway, platelet-derived growth factors and their receptors (PDGF/PDGFR) pathway [6], fibroblast growth factors and their receptors (FGF/FGFR) pathway [7], angiopoietins and their receptors(ANG/TIE) [8], hepatocyte growth factor and its receptor (HGF/MET) [9] are all responsible for angiogenesis and designated as targets of tumor treatment. In addition, pro-inflammatory factors such as interleukins produced by tumor cells infiltrated immune cells and stromal cells also play dual roles in the blood vessel formation event. For instance, IL-1 induces and maintains angiogenesis by activation of tumor infiltrating cells to produce endothelial cell activating factors like VEGF [10], and IL-35 enhances angiogenesis by increasing the numbers of CD11b+Gr1+ myeloid cells in tumors [11]. On the contrary, interleukins that exhibit negative effects on tumor blood vessel formation include IL-4 and IL-24 by inhibition of basic fibroblast growth factor (bFGF) induced endothelial cells migration [12, 13] and IL-12 by induction of T cell to produce IFN-γ [14].

In addition to tumor cells, *per se*, a variety of immune cells participate in the initiation, progression and metastasis of solid tumors [15]. Accumulating studies indicate that the most notable cell types in the tumor microenvironment are immune

cells [1]. Tumor-associated macrophages (TAMs) are important regulators of tumorigenesis that are either tissue-resident, or in the peripheral circulating system, mainly originated from the bone marrow. Macrophages have inherent plasticity, in which they are polarized into classically activated macrophages (M1) or alternatively activated macrophages (M2) by different mediators [16]. M1 macrophages are mainly polarized by stimulation with Interferon-γ (IFN-γ), lipopolysaccharide (LPS) and granulocyte-macrophage colony-stimulating factor (GM-CSF). They produce pro-inflammatory cytokines and phagocytose a variety of pathogens and intracellular bacteria. CD80, CD68 and inducible nitric oxide synthase (iNOS/NOS2) are defined as M1 macrophage markers [17]. M2 macrophages are polarized by stimulation with interleukin (IL)-4, IL-10, IL-13 and other factors. In mice, M2 macrophage markers include arginase 1 (Arg-1), chitinase 3-like 3 (also known as YM1), and macrophage mannose receptor 1 (also known as CD206) [18]. M2 macrophages play a central role in parasite responses, tissue remodeling, angiogenesis and pro-tumoral activity.

1.2 Granulocytes in tumors

Granulocytes, which are another essential immune cell population, consist of three types: neutrophils, basophils and eosinophils. Neutrophils have been reported to display phenotypical plasticity in tumors, presenting anti-tumorigenic (N1) or pro-tumorigenic (N2) functions [19]. Pro-tumorigenic neutrophils, which were reported to be polarized by the presence of transforming growth factor-β (TGF-β) [20], promote angiogenesis, tumor progression and metastasis [19, 21-23]. On the other hand, interferon-β (IFN-β) induced anti-tumorigenic neutrophils and blocked tumor progression by inhibiting angiogenesis [24] and the release of pro-inflammatory mediators [25].

Basophils have been focused because of their positive role in angiogenesis and inflammation through the vascular endothelial growth factor (VEGF) and their

receptors [26]. Additionally, basophils contributed to tissue remodeling through the IgE/tumor necrosis factor-α (TNF-α)/matrix metalloproteinase-9 (MMP-9) axis [27].

Eosinophils that infiltrate tumors, which are also termed tumor-associated tissue eosinophils (TATEs), were also reported to have dual function. Mice with completely eosinophil deficiency exhibited increased tumorigenicity in association with reduced TATEs [28], whereas tumor-associated eosinophils could be recruited and licensed to promote the growth of cervical cancer cells by thymic stromal lymphopoietin [29]. A variety of studies have shown that eosinophils are attracted into tumors by chemotactic factors [28] such as eotaxin. However, the role of tumor-associated eosinophils is not clear. Some clinical research demonstrated that in the gastrointestinal cancers, head and neck cancer, bladder cancer and prostate cancer [30] the eosinophils were over-accumulated and would be designated as a good prognosis. On the other hand, in regard to oral squamous cell carcinoma and cervical carcinoma, eosinophils were related to a poor predict marker [30, 31]. Recently, a research focused on the eosinophils relation with the tumor immunity [32]. The eosinophils supported tumor rejection, but only when the eosinophils were activated and tumor-specific CD8 positive T cells presented. Under these conditions, activated eosinophils improved the infiltration of T cells into the tumor by creation of a tumor microenvironment, which enhanced tumor rejection and survival.

1.3 The differences between MS-K and NFSA tumor cells

By previous research, we found that there are some differences between tumors formed by mouse sarcoma cell line NFSA and MS-K [33]. Both cells can form large-volume tumors. However, NFSA tumors formed necrotic cores, whereas MS-K tumors formed well developed blood vessel network. Moreover, NFSA tumor can recruit more CD14+ cells than MS-K tumor. CD14 positive cells mainly consist of monocytes and macrophages which can mediate the inflammatory response. These

differences promoted us to examine the gene expression profile differences between these two cell lines [34]. By performing DNA microarray, it was seen that interleukin *il18* and C-C chemokine ligand *ccl11* were highly expressed in NFSA cells (**Figure 1**).

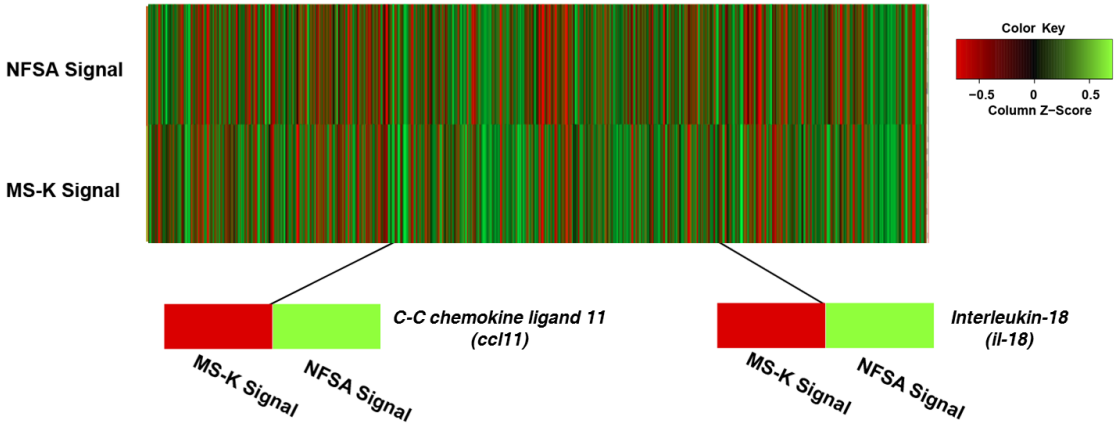

Gene name	Log2(MS-K/NFSA)
Mus musculus interleukin 18 (*il18*)	-5.06
Mus musculus chemokine (C-C motif) ligand 11 (*ccl11*)	-10.54

Figure 1. DNA microarray analysis of gene profile in the MS-K and NFSA cells.

The microarray data was analyzed by an application Multi Experiment Viewer (MeV).

Moreover, another previous research demonstrated that NFSA tumor derived IL-18 induced macrophages into M1 type, destructed endothelial cells *in vitro* by induction of NO and may result in NFSA tumor necrosis by enhancing phagocytosis and cytotoxicity of macrophages [34]. Thus, it is critical to examine whether ectopic expression of IL-18 in MS-K tumors inhibits angiogenesis and tumor growth *in vivo*.

In further, infiltrated granulocytes were also examined in NFSA and MS-K tumors. The ratio of the infiltrated CD14+Gr-1+ cells (designated as granulocytes) was examined in the MS-K and NFSA tumors by flow cytometry. The CD14+Gr-1+ cell ratio in the NFSA tumors were significantly higher than in the MS-K tumors (**Figure 2**). Moreover, all pro-inflammatory genes were highly expressed in the CD14+Gr-1+ cells from the NFSA tumors. These pre-research results indicated that the tumor infiltrated CD14+Gr-1+ cells might contribute to the tumor necrosis.

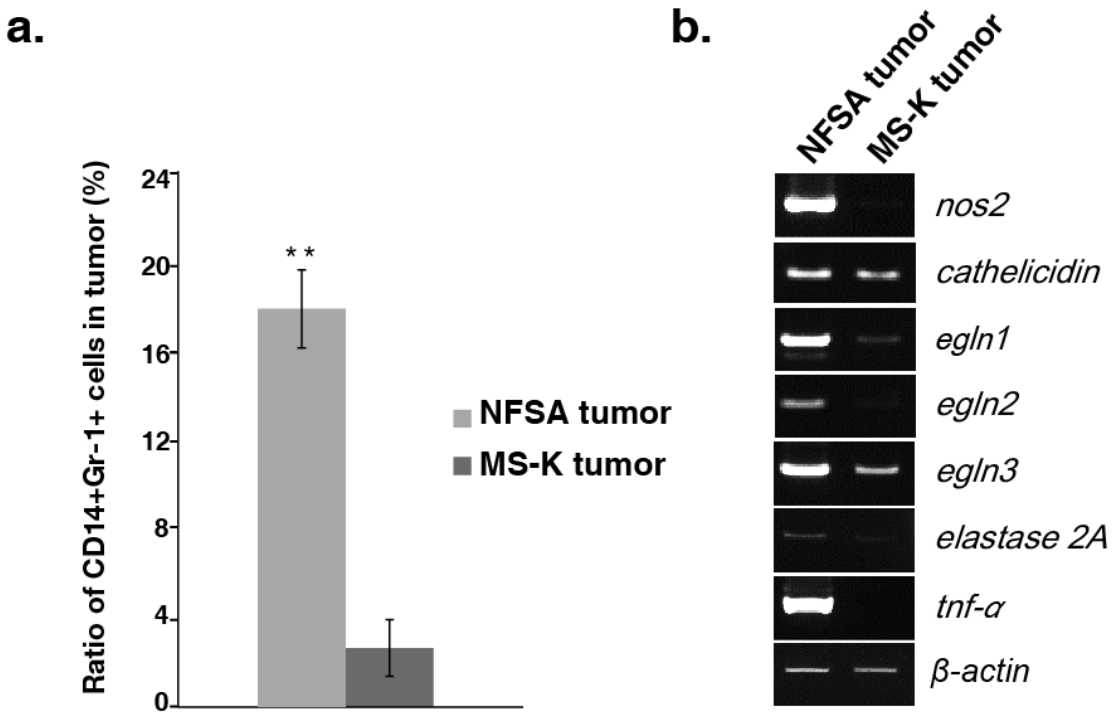

Figure 2. The CD14+Gr-1+ cells infiltration in the NFSA and MS-K tumors.

a. The ratio of CD14+Gr-1+ cells in the NFSA and MS-K tumors were examined by flow cytometric analysis. The data represents the average ± standard deviation (n = 3).

b. RT-PCR analysis revealed the gene expression profile of the CD14+Gr-1+ cells in the NFSA and MS-K tumors.

As a C-C motif chemokine family member, CCL11 was notably reported to be responsible for recruiting the eosinophils [35, 36]. CCL11 also exhibits an inhibitory role in the differentiation of dendritic cells (DCs) and enhances Th2-polarization [37]. The biological effects of CCL11 are mediated via CC chemokine receptor 3 (CCR3) [38], which is highly expressed on eosinophils and other cells. CCL11 and CCR3 were determined to be key mediators in the accumulation of eosinophils and in the production of fibrogenic cytokines [39]. CCL11 signaling plays an important role in proliferation and invasion of ovarian carcinoma cells [40]. Although CCL11 has been related to diseases associated with eosinophils infiltration [41], its role in the tumor formation and angiogenesis remains unclear.

1.4 Overview of this research

In the present study, MS-K-IL-18 clones and MS-K-CCL11 were established to examine the role of IL-18 and CCL11 in tumorigenesis and angiogenesis.

The MS-K-IL-18 clones were subcutaneously inoculated into the mice. Blood vessel formation in these MS-K-IL-18 tumors was less than the parental MS-K tumor and more accumulation of M1 macrophages in the MS-K-IL-18 tumor was observed. Furthermore, the IL-18-stimulated macrophages induced apoptosis of endothelial cells. Thus the excess IL-18 inhibited tumor blood vessel formation *in vivo*.

For CCL11, CCL11 overexpressing MS-K clones (MS-K-CCL11) were established, characterized and were subsequently inoculated subcutaneously into C3H/HeN mice as well. However, no tumors were formed by the MS-K-CCL11 clones. As a chemokine ligand, the role of the CCL11 in the eosinophil migration was confirmed by a transwell assay and its effect on eosinophil induction from bone marrow (BM) cells was demonstrated. Moreover, a co-culture assay was carried out to examine the BM-derived eosinophils effects on the endothelial cells and tumor cells. On the other hand, the CCR3 antagonist was administrated during the NFSA tumor formation and its effect on eosinophil infiltration and angiogenesis were also examined in further. The overview was made into a chart (**Figure 3**).

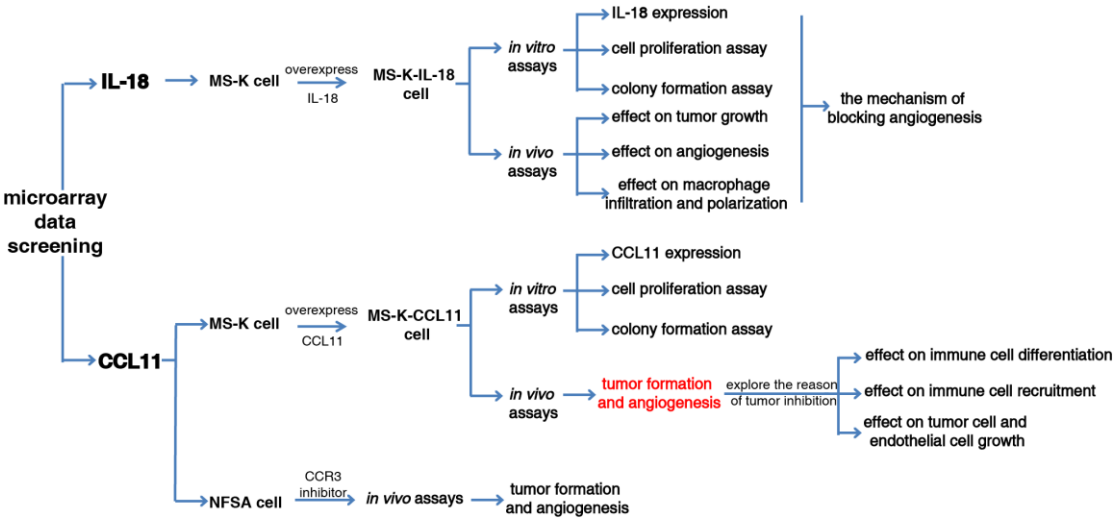

Figure 3. The overview chart of this research.

2. Materials and Methods

2.1 Mice

The C3H/HeN strain mice were purchased from SLC (SLC Co. Ltd, Sizuoka, Japan) and bred in specific pathogen-free condition (SPF). Eight to 12-week-old C3H/HeN mice were used in all the experiments. Animal experiments were carried out according to the guidelines of animal experiments of Niigata University.

2.2 Cells

Maintenance of normal MS-K and NFSA cell line was described previously [34]. Maintenance of the IL-18 overexpressing MS-K clones and the CCL11 overexpressing MS-K clones was carried out with alpha-modified minimal essential medium (α-MEM) supplemented with 5% (v/v) horse serum (HS). The murine monocyte/macrophage cell line RAW 264 [42] was obtained from the American Type Culture Collection (ATCC, Rockville, MD, USA) and maintained in Dulbecco's modified Eagle's medium (DMEM) (Gibco, CA, USA) supplemented with 10% (v/v) fetal bovine serum (FBS) and 2 mM L-glutamine. The murine endothelial cell line F-2-Kusabira Orange [34] was cultured in RPMI-1640 (Gibco, CA, USA) supplemented with 5% FBS. All medium contained 100 U/mL penicillin and 100 μg/mL streptomycin (GIBCO). Cells were cultured at 37°C in humidified atmosphere in 5% (v/v) CO_2-incubator.

2.3 Construction of pIRES2-IL-18-ZsGreen1 and pIRES2-CCL11-ZsGreen1

Coding sequence of mature IL-18 and CCL11 protein was amplified by PCR using the PrimeStar max DNA polymerase (Takara, Tokyo, Japan) using NFSA cDNA as template with forward and reverse primer (**Supplemental Table 1**). Then the PCR products were directionally cloned into the *Nhe* I / *Xho* I site of the pIRES2-ZsGreen1

vector (CLONTECH Inc., CA, USA) respectively. The mock vector contains no transgene in the expression cassette.

2.4 Establishment of MS-K-IL-18 and MS-K-CCL11

MS-K cells were transfected with the pIRES2-IL-18-ZsGreen1 vector and pIRES2-CCL11-ZsGreen1 vector, and then medium was replaced by the medium with geneticin (400 μg/mL) to perform antibiotic selection. The survived cells, which expressed the ZsGreen1 fluorescent protein, were sorted by FACS Aria II (BD, Tokyo, Japan) to make single clones. Several ZsGreen1-expressing clones for IL-18 and CCL11 were picked up to check the expression of the *il-18* or *ccl11* by quantitative PCR (qPCR). Then the five *il-18*-overexpressing MS-K clones (MS-K-IL-18) and five *ccl11*-overexpressing MS-K clones (MS-K-CCL11) were established.

2.5 Analysis of gene expression by RT-PCR and qPCR

Preparation of the cDNA from cultured cells or tumor-derived cells was described in previous paper [34]. The qPCR was performed to measure the expression level of *il-18* and *β-actin* in the MS-K-IL-18 clones using the Light Cycler (Roche Diagnostics GmbH, Manheim, Germany). Then the relative expression of the *il-18* against *β-actin* was calculated. Similarly, *ccl11* relative expression to *β-actin* was also checked in the MS-K-CCL11 clones.

In some experiment, the expression of and β-actin was analyzed by RT-PCR with gene-specific PCR primers. Briefly, the reaction was carried out using 2×GoTaq® Green Master Mix (Promega, CA, USA), forward primers and reverse primers, diluted cDNA template and distilled water. The PCR products were analyzed by electrophoresis in a 2% agarose gel containing proper concentration of ethidium bromide. The sequences of primers were summarized in **Supplemental Table 1**.

2.6 Cell proliferation assay

The MS-K-IL-18 clones and MS-K-CCL11 clones were seeded in 35 mm culture dish at the density of $1x10^4$ cells/dish. Appropriate controls were included in the experiment. The number of living cells was counted by trypan blue dye exclusion test from day 2 to day 5.

2.7 Colony formation assay

The MS-K-IL-18 clones or MS-K-CCL11 clones (1×10^3 cells) were seeded in the medium supplemented with 0.8% methylcellulose in 35m/m dish (Falcon #1008, BD, Tokyo, Japan) and incubated at 37 °C in 5% CO_2 incubator. Appropriate controls were included in the experiment. Four parallel experiments for each cell clone were performed. Number of colonies was counted on day 12.

2.8 Confocal microscope observation of MS-K overexpressing clones

Proper number of the MS-K-IL-18 cells were suspended in the culture medium and seeded onto the bottom glass dishes (IWAKI glass, Tokyo, Japan) and incubated at 37 °C for 72 hours. Then the cells were rinsed with phosphate-buffered saline (PBS) and fixed with formalin phosphate buffer for 30 minutes. After blocking and permeabilization with 0.3% (v/v) bovine serum albumin (BSA), 0.05% Tween-20-PBS for 1 hour at room temperature, the cells were incubated with anti-IL-18 antibody (1:1000 dilution with 0.3% goat serum/PBS, Sigma Aldrich Japan, Hokkaido, Japan) overnight. After washing with PBS, the cells were incubated with Hilyte Plus 555 labeled anti-rabbit IgG antibody (1:1000 dilution with 0.3% goat serum/PBS, AnaSpec, CA, USA) for 1 hour and counterstained with the 4′,6-diamidino-2-phenylindole (DAPI; Invitrogen, Tokyo, Japan) before observation. For MS-K-CCL11 clones, the protocols

were same as above described, besides the first antibody was anti-CCL11(1:1000 dilution with 0.3% (v/v) goat serum/PBS, Biolegend, CA, USA) and the second antibody was Alexa Fluor 647 labeled anti-rat IgG antibody (1:1000 dilution with 0.3% (v/v) goat serum/PBS, Biolegend, CA, USA). The observation was done by the confocal laser scanning microscope (Leica, Wetzlar, Germany). Appropriate blanks and controls were included in the experiment.

2.9 Quantification of IL-18 and CCL11 in the CM of overexpressing clones

NFSA, MS-K, MS-K-mock, MS-K-IL-18 clones, MS-K-CCL11 clones were culture for three days to prepare the conditioned medium. The concentrations of IL-18 in the conditioned media (CM) were determined using mouse IL-18 ELISA kit (MBL, Tokyo, Japan) according to the manufacturer instructions. The CCL11 concentrations in the CM were quantified using a Mouse Eotaxin Platinum ELISA kit (eBioscience, CA, USA).

2.10 Tumor formation assay

For CD14+ and CD14+Gr-1+ cells analysis, MS-K, NFSA cells and MS-K-IL-18 clones were respectively (n=3) administered subcutaneously into C3H/HeN mice at 1 × 10^6 cells/site and incubate for 30 days. For Siglec-F+Gr-1+ cells analysis, NFSA cells were administered subcutaneously into C3H/HeN mice and incubate for 18 days.

2.11 immune cells infiltration analysis in the tumors

The tumors were excised and single cell suspension was prepared by mechanically cut and collagenase (Yakuruto, Tokyo, Japan) treatment. In detail, at first, the mice were sacrificed and tumors were excised from mice and weights were measured. For one sample, about 500 mg tumor was taken into a 50 mL plastic

centrifuge tube containing 0.5 mL HBSS. Then the tumor was cut into small pieces using the big scissors. The collagenase solution (3 mL/tumor, 250 units/mL) were directly added to the cell suspension and incubated at 37 °C in the water bath for 30 minutes with gentle shaking. Then the cell suspension was passed through the sterile metal mesh to remove the big tumor blocks. Then the cells were washed with the FACS buffer (2%FBS/PBS) twice. Then the cell suspension was filtrated with nylon mesh (#200 mesh, J-Medical, Niigata, Japan) and the cell number was counted using Türk solution. Designated number of cells was added into a centrifuge tube, and after centrifuge, the supernatant was removed. Then, to block the non-specific binding of the antibody to Fc receptor, about 2 mL of the conditioned medium of 2.4G was added to the cells and incubated on ice for 10 minutes. Then cells were washed again with the FACS buffer (2%FBS/PBS) twice, and dispensed into the six 1.5 mL centrifuge tubes. #1: the negative control, only stained by Propidium iodide (PI); #2: the phycoerythrin (PE)-conjugated anti-Gr-1 antibody staining (1 μL/10^6 cells, 1/100 diluted with FACS buffer, Biolegend, CA, USA); #3: the allophycocyan (APC)-conjugated anti-CD14 antibody staining (1 μL/10^6 cells, 1/100 diluted by FACS buffer, Biolegend, CA, USA) ; #4: the APC-conjugated anti-mouse Siglec-F (1 μL/10^6 cells, 1/100 diluted by FACS buffer, Miltenyi Biotec, CA, USA) staining; #5: the PE-anti-Gr-1 antibody and APC-anti-CD14 antibody and PI staining; #6: the PE-anti-Gr-1 antibody, APC-anti-Siglec-F antibody and PI staining. Then cells were treated with each antibody except PI for 30 minutes at 4°C in fridge. Following the washing with the FACS buffer (2%FBS/PBS) twice, appropriate volume of the FACS buffer were added to the cell suspension and the PI solution was added. Then the cells were passed through the filter. Cell analysis and sort were carried out by FACS Aria II (BD, Tokyo, Japan).

2.12 Differentiation of eosinophils by CCL11-stimulation

The BM cells were prepared from the femurs and tibias of the C3H/HeN mice. Appropriate numbers of the BM cells were suspended in the Dulbecco's modified Eagle's medium (Gibco, CA, USA) that was supplemented with 0.8% (v/v) methylcellulose (NACALAI TESQUE, INC., Kyoto, Japan), 10% (v/v) FBS and additional protein factors. Recombinant granulocyte colony-stimulating factor (G-CSF, final conc. 30 ng/mL, Chugai Pharmaceutical Co. Ltd, Tokyo, Japan), recombinant CCL11 (rCCL11, Biolegend, CA, USA), parental MS-K- CM and MS-K-CCL11-CM were used as the protein factors. After 7 days, the cells were harvested and analyzed by FACS.

2.13 Transwell migration assay

A transwell assay was performed to evaluate the migration activity of the eosinophils. Briefly, BM cells were stimulated with MS-K-CCL11-CM in semi-solid media for 7 days to induce the eosinophils. The stimulated BM cells ($1x10^5$ cells) were applied onto the upper chamber of the transwell (pore size 8 μm, BD, Tokyo, Japan), then the transwell chambers were placed in a 24-well plate, which contained MS-K-CCL11-CM, parental MS-K-CM, and MS-K-mock-CM. Medium that was supplemented with 5% HS was used as a negative control, and medium supplemented with 100 ng/mL of recombinant CCL11 was used as a positive control. After 90 minutes of culture, the cells beneath the inserts were fixed and stained with crystal violet solution. Then, the area covered by the stained cells was measured with ImageJ software (U.S. National Institutes of Health), and the area of the MS-K-CM group wells was set to 1.

2.14 Co-culture of induced eosinophils and tumor or endothelial cells

To check the cytotoxicity level of the induced eosinophils, a co-culture with tumor or endothelial cells was performed. Briefly, MS-K-GFP, NFSA-GFP and F-2-Kusabira orange cells were seeded in dishes at the appropriate density to make monolayers. After 24 hours, the BM cells that were stimulated with MS-K-CCL11-CM or MS-K CM were seeded on the monolayer at various ratios (1:10, 1:1, 1:0.1), respectively. After 48 hours, the photographs were taken, and the cell suspension was prepared. The number of living cells was analyzed using FACS by PI staining.

2.15 CCR3 antagonist injection into NFSA tumor-bearing mice

The NFSA cells ($1x10^6$ cells/mouse) were injected subcutaneously into the right abdomen region of C3H/HeN mice on day 0. The mice were subsequently randomized to receive different doses of specific CCR3 antagonist SB 328437 (1 mg/kg, n=3; and 5 mg/kg, n=3; Abcam, Tokyo, Japan), or vehicle alone (PBS, n=3) by intraperitoneal injection consecutively from day 5 to day 18. Tumors were excised on day 18 for eosinophil infiltration analysis and blood vessel formation analysis by anti-CD31 immunohistochemical staining.

2.16 Immunohistochemical staining of paraffin-embedded tumor sections

For staining blood vessels, immunohistochemical staining with anti-CD31 antibody was carried out according to the previous report [33]. Briefly, paraffin embedded tumors were prepared and 4μm tumor sections were sliced, dehydrated and boiled for 15 minutes in 100 mM Tris-HCl (pH10.0). Anti-CD31 antibody (AnaSpec, CA, USA) was used as the first antibody. For labelling first antibody, the peroxidase-conjugated secondary antibody (KPL, MD, USA) and the diaminobenzidine (DAB) solution (VECTOR laboratories, CA, USA) were employed.

Then, the nuclei were counterstained with hematoxylin. Microvessel density was quantified by counting the number of CD31 positive staining structures of different length range in five random fields in the tumor sections. For VE-cadherin staining, the sections were treated with anti-VE-cadherin antibody (Santa Cruz Biotechnology, Texas, USA) and Hilyte Plus 555-labeled anti-goat IgG antibody (AnaSpec, CA, USA) and DAPI. The observation was done by the confocal laser scanning microscope (Leica, Wetzlar, Germany). Appropriate blanks and controls were included in the experiment.

For eosinophil staining, anti-Siglec-F antibody was used to treat the tumor section at first. After washing with PBS, the sections were treated with FITC labeled anti-rat IgG antibody (Jackson ImmunoResearch, PA, USA) and DAPI. The observation was done by the confocal laser scanning microscope (Leica, Wetzlar, Germany). Appropriate blanks and controls were included in the experiment (data not shown).

2.17 Statistical analysis

All results present as means ± SD. For statistical analysis, Student t-test was applied in data analysis. In all figures, * means $p < 0.05$, and ** means $p < 0.01$, and *** means $p < 0.001$, respectively.

3. Results

3.1 The function of IL-18 on MS-K tumor formation and angiogenesis

The IL-18 was overexpressed in the MS-K cells, which expressed low level of IL-18, and the IL-18 overexpressing clones were used to check the IL-18 effect on tumor formation and angiogenesis *in vivo.*

3.1.1 The establishment of IL-18 overexpressing MS-K clones

At first, the IL-18 expression vector using modified pIRES2-ZsGreen1 vector was constructed. The mature IL-18 coding sequence was amplified and cloned into the EF1α promoted-pIRES2-ZsGreen1 vector. Then the vector was transfected into parental MS-K cells. By antibiotic selection and single cell sorting using flow cytometry, five IL-18 overexpressing MS-K clones (MS-K-IL-18) were primarily selected by fluorescence (**Figure 4**). At the same time, MS-K-mock clone which contained blank pIRES2-ZsGreen1 vector was also established.

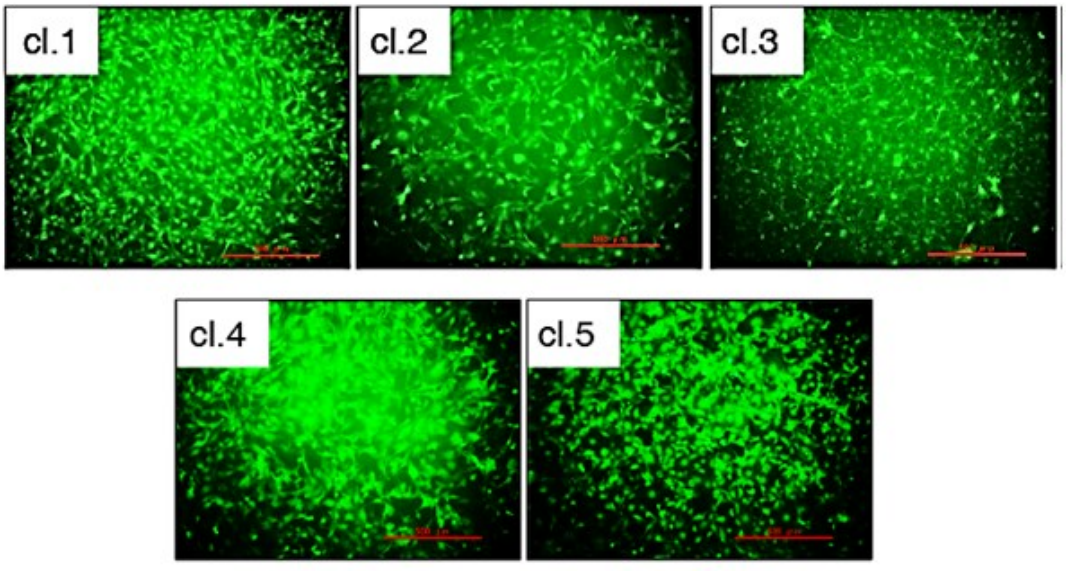

Figure 4. Primary selection of five MS-K-IL18 clones by fluorescence.

These five clones were selected by their strong expression of ZsGreen1.

Secondly, RT-PCR and quantitative PCR were performed to examine the *il-18* expression level. The *il-18* was highly expressed in the 5 clones, compared to parental MS-K cells and NFSA cells (**Figure 5a**). Moreover, The MS-K-IL-18 clones showed higher expression levels of *il-18* receptor *il-18r1* than the NFSA cell line. The expression of *il-18 receptor accessory protein* (*il-18 rap*) and *vegf-A* was not changed between the parental MS-K and MS-K-IL-18 clones. By quantitative PCR result (**Figure 5b**), *il-18* expression level was confirmed in further. Because the *il-18* expression level was top in the MS-K-IL-18 cl.1 and cl.5, so these two clones were sequentially used in the following assays.

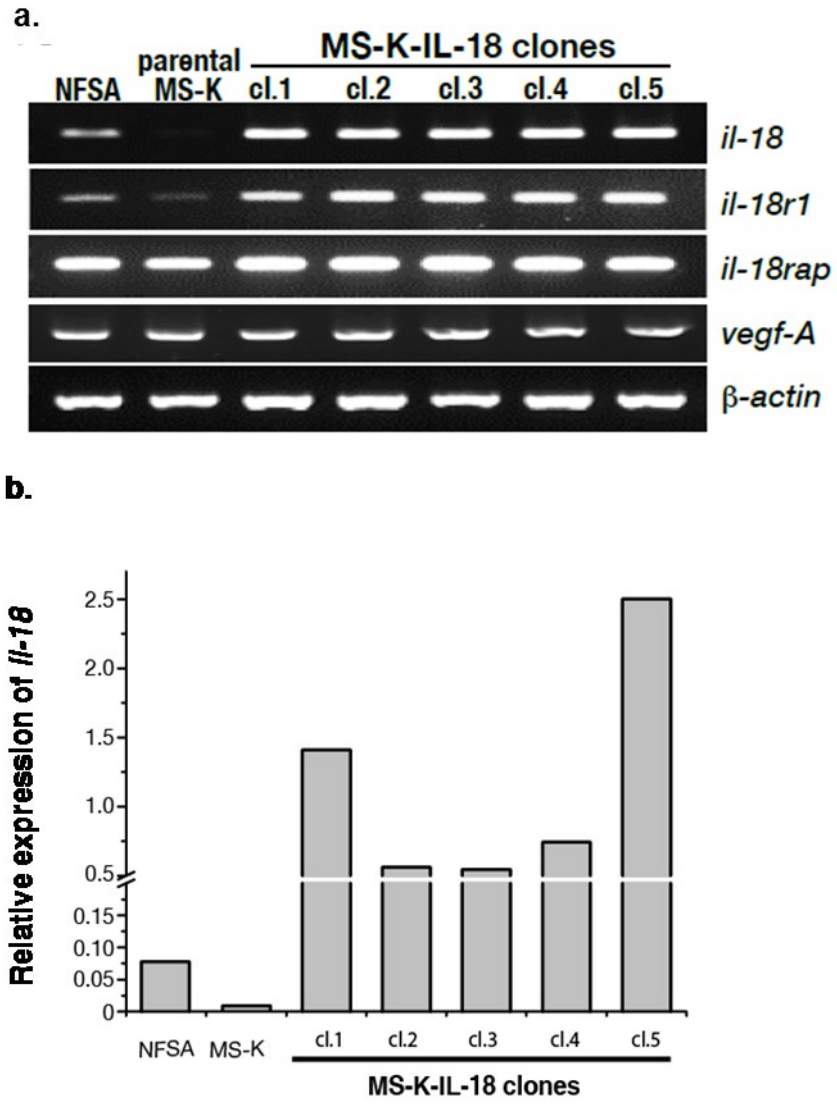

Figure 5. The *il-18* expression in the MS-K-IL-18 clones.

a. The expression of *il-18, il-18 r1, il-18 rap* and *vegf-A* in the MS-K-IL-18 clones was analyzed by RT-PCR.

b. Relative expression of *il-18* (*il-18*/*β-actin*) in the MS-K-IL-18 clones was measured by qPCR.

3.1.2 The protein expression in the MS-K-IL-18 clones

IL-18 protein expression in MS-K-IL-18 clones was then examined by confocal microscope observation stained with anti-IL-18 antibody (**Figure 6**). The Hilyte plus 555 labelled second antibody signal distributed in the cytoplasm of the MS-K-IL-18 cells, indicating the IL-18 protein expression in the cytoplasm.

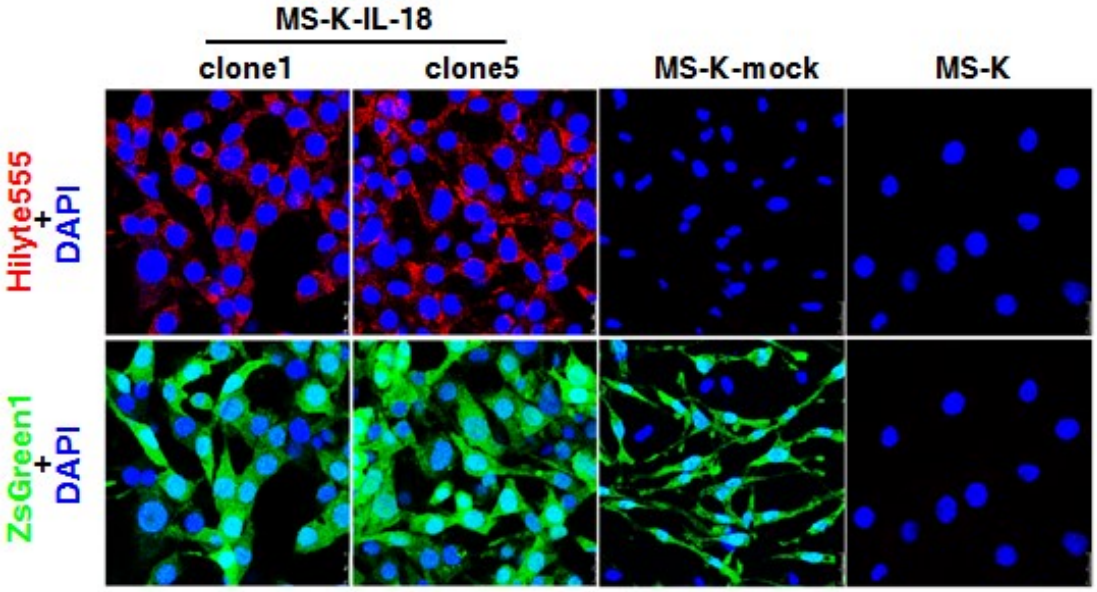

Figure 6. Confocal microscope observation of the expression of IL-18 in MS-K-IL-18.

Hilyte555 merged with DAPI indicated the IL-18 distribution, and the ZsGreen1 merged with DAPI indicated the cell shape of the MS-K-IL-18 clones.

Moreover, the ELISA assay was performed to quantify the IL-18 concentration in the conditioned medium of the MS-K-IL-18 clones compared to parental MS-K, MS-K-mock and NFSA.

Table 1 IL-18 quantification in the MS-K-IL-18-CM

Sample name	Concentration of IL-18 in the CM (pg/mL)
Parental MS-K	30.63 ± 2.69
MS-K-mock	29.69 ± 6.20
MS-K-IL-18 cl.1	1524.39 ± 25.01
MS-K-IL-18 cl.5	2184.38 ± 25.01
NFSA	483.68 ± 51.73

3.1.3 The characterization of MS-K-IL-18 clones *in vitro*

In the following, the characteristics of the MS-K-IL-18 were examined *in vitro.* Firstly, a cell proliferation assay was carried out to check the MS-K-IL-18 clone proliferation rate compared to parental MS-K cells and MS-K-mock cells.

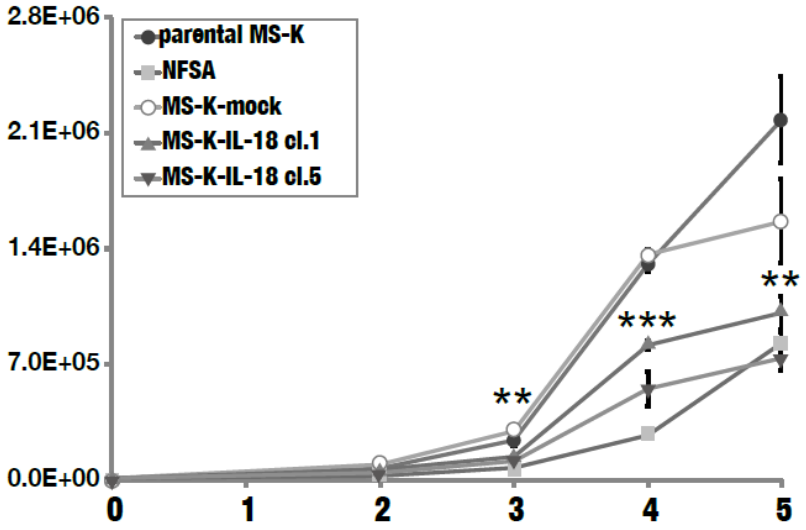

Figure 7. Growth curve of MS-K-IL-18 clones.

The cell number was counted on day 2 to day 5. Data indicated mean ± standard deviation (n = 3). ** indicates $p < 0.01$, and *** indicates $p < 0.001$.

The cell proliferation assay showed the MS-K-IL-18 clones grew slower than parental MS-K and MS-K-mock clone (**Figure 7**).The colony formation assay showed

there were no significant differences of colony numbers between the parental MS-K and the MS-K-IL-18 clones (**Figure 8a**). However, the colony size of the MS-K-IL-18 clones was apparently reduced (**Figure 8b**).

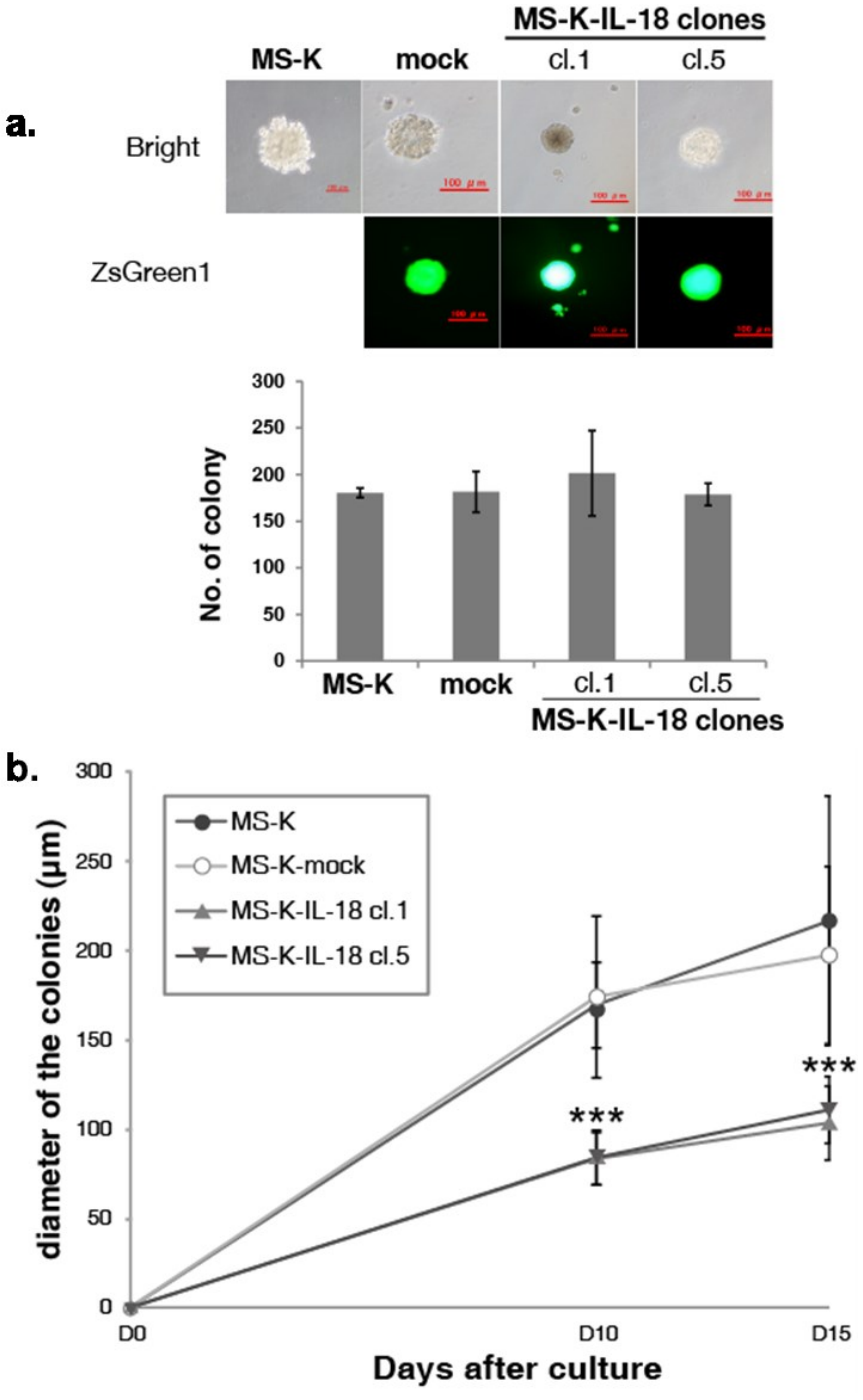

Figure 8. The colony formation analysis for MS-K-IL-18 clones.

a. The photos of the colonies were taken on day 15. The colony numbers were counted on day 15 and the data indicated mean ± standard deviation (n = 4).

b. The diameters of the colonies for each cell were measured on day 10(D10) and day 15 (D15). Data indicated mean ± standard deviation (n = 4). *** indicates $p < 0.001$.

3.1.4 The effect of IL-18 on tumor formation and angiogenesis

To check IL-18 function in tumors, MS-K-IL-18 clones and normal MS-K cells were subcutaneously inoculated into mice.

To evaluate the function of IL-18 in tumors, the MS-K-IL-18 clones and parental MS-K cells were subcutaneously inoculated into mice. After 30 days growth, the tumors were excised (**Figure 9**). There were no significant differences in tumor weight (MS-K: 2.09 ± 0.08 g, MS-K-IL-18 cl.1: 1.88 ± 0.98 g, MS-K-IL-18 cl.5: 1.36 ± 0.92 g) (n=3).

By the photos of the tumors, the blood vessels were enriched in the parental MS-K cells formed tumors; however, in the MS-K-IL-18 clones formed tumors, the blood vessels were barely seen in the inner core of the tumors.

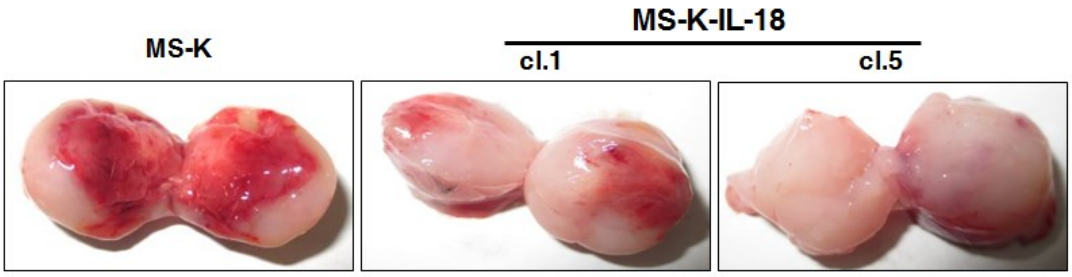

Figure 9. The effect of Il-18 on tumor formation.

An immunohistochemical staining demonstrated there was poor blood vessel formation in the MS-K-IL-18 tumors, contrary to enriched blood vessels in the parental MS-K tumors (**Figure 10a**). The length of the formed blood vessels was obviously

shorter in the cl. 5 tumors compared with parental MS-K tumors (**Figure 10a**). Necrotic area was observed in the core of cl. 1, because of failure of blood vessels. To quantify blood vessel density, the numbers of CD31 positive staining structures of different lengths in the parental MS-K and MS-K-IL-18 cl.5 tumor sections were calculated (**Figure 10b**). Blood vessels in the MS-K-IL-18 tumors were mainly distributed at the range of shorted than 10 μm and there were no blood vessels longer than 50 μm. In contrast, there were similar numbers of different length blood vessels in the parental MS-K tumors. Furthermore, the confocal microscope observation of fluorescent- immunohistochemical staining using anti-VE-cadherin antibody confirmed that there were no signals of blood vessels in the MS-K-IL-18 tumors compared to the parental MS-K tumors (**Figure 10c**).

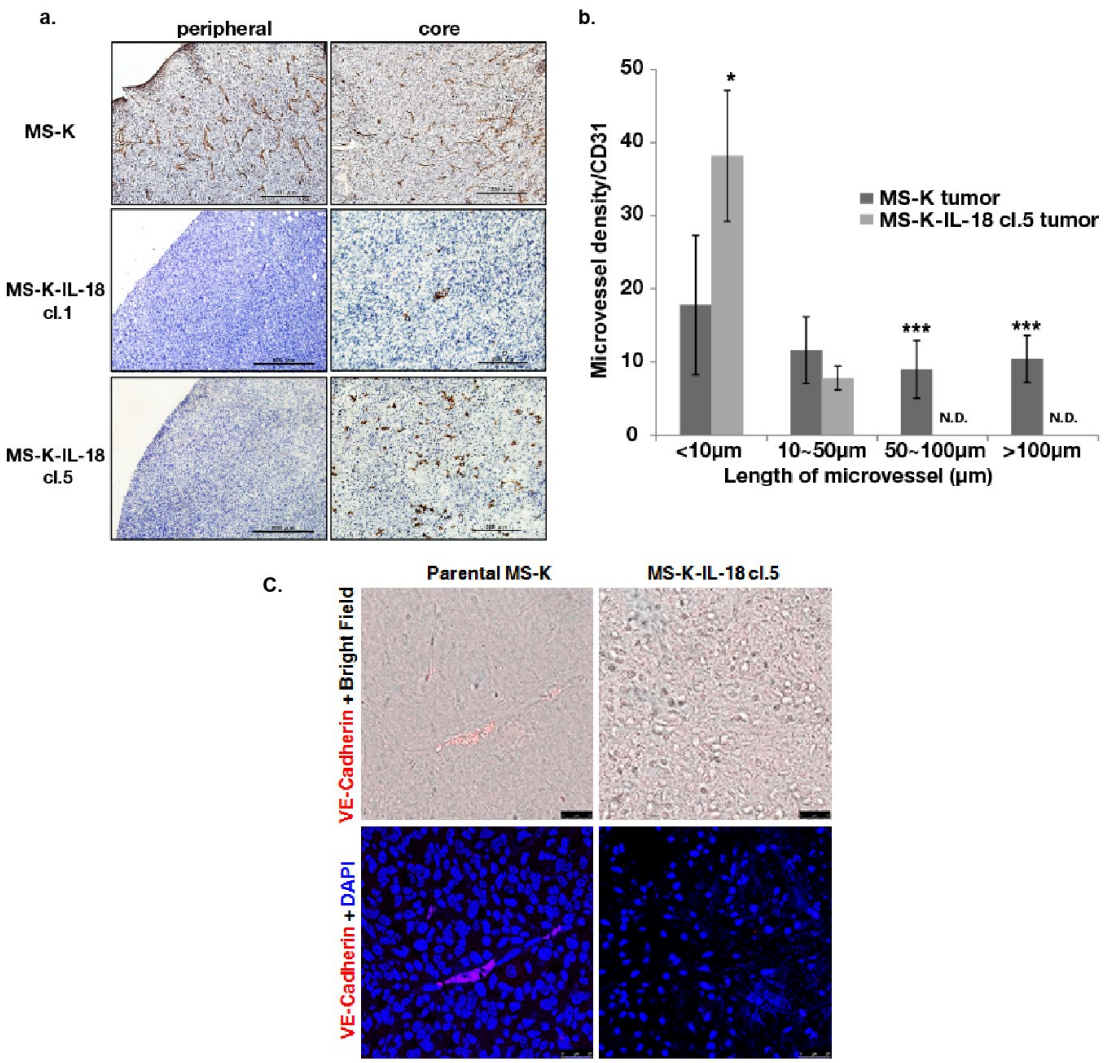

Figure 10. The effect of IL-18 on tumor angiogenesis.

a. Immunohistochemical staining of parental MS-K and MS-K-IL-18 clone tumor sections was performed using anti-CD31 antibody. The brown area means the CD31-positive blood vessels. The small photograph in e showed the necrotic area in the tumor.

b. The microvessel diversity was calculated in parental MS-K and MS-K-IL-18 (cl.5) tumors. * indicates $p < 0.05$ and *** indicates $p < 0.001$.

c. Anti-VE-cadherin antibody staining was performed and the confocal microscope observation was performed. Red area means the VE-cadherin+ blood vessels. Bar is 25μm.

3.1.5 The effect of IL-18 on immune cells infiltration and polarization

After tumor excision, some tumors were cut up and treated with collagenase into single cells. Then immune cells infiltration was analyzed using flow cytometry (**Figure 11**). The result demonstrated that the ratio of the CD14+ cells in the MS-K-IL-18 cl. 5 was less than in parental MS-K tumors, but the ratio of the CD14+ cells in the MS-K-IL-18 cl. 1 was not significantly changed.

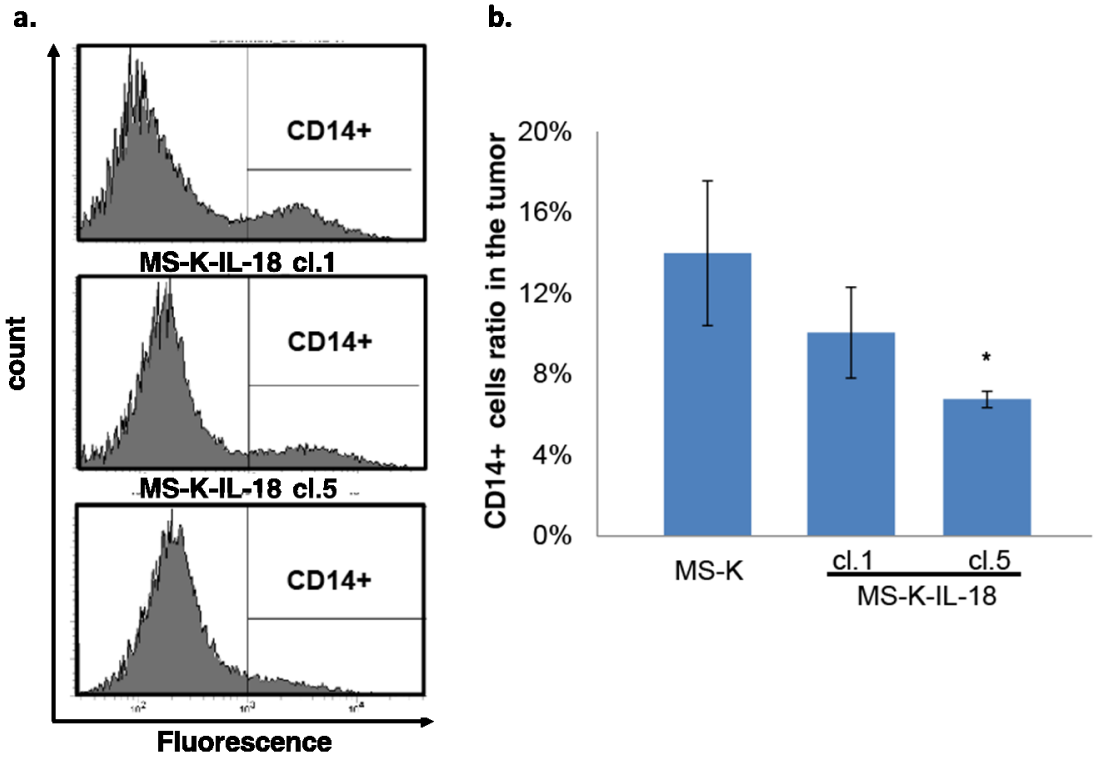

Figure 11. The effect of IL-18 on CD14-positive cells infiltration.

a. APC labelled-CD14- positive cells were analyzed according to the fluorescence of APC.

b. The average percentage of CD14- positive cells was calculated. * indicates $p < 0.05$.

Then the CD14-positive cells were sorted using the flow cytometry and the RNA was extracted from the cells. The expression of macrophage markers was checked in the tumor derived CD14-positive cells using RT-PCR (**Figure 12a**). The expression of the M1 macrophage marker *il-6* was obviously induced in the CD14+ cells derived

from MS-K-IL-18 tumors. Conversely, the expression of the M1 marker *nos2* and *cd86*, and M2 marker *il-10* and *mrc1* was not affected in the CD14+ cells derived from MS-K-IL-18 tumors.

Moreover, to confirm the M1 macrophage infiltration, the M1 macrophage ratio was also analyzed using anti-CD11b and anti-CD80 antibodies. The CD11b+CD80+ M1 macrophages accumulated significantly in the MS-K-IL-18 cl.1 and cl.5 tumors (**Figure 12b, c**). These results indicated that the IL-18 could induce the M1 macrophage in the MS-K tumor.

3.1.6 The effect of IL-18 stimulated macrophage on endothelial cells

To explain the reason of the inhibition of angiogenesis in the MS-K-IL-18 tumors, the stimulated murine macrophage cell line RAW264 cells were co-cultured with murine endothelial cell line F-2-Kusabira Orange (F-2-KO) cells for 48 hours. Then apoptotic analysis was carried out using Annexin-V and propidium iodide double staining (**Figure 13a**) .The RAW264 cells stimulated with the conditioned medium of MS-K-IL-18, NFSA, or with rIL-18, damaged the F-2-KO cells (**Figure 13b**) and increased the ratio of early apoptotic F-2-KO cells and terminal apoptotic F-2-KO cells, compared to the MS-K-CM stimulation (**Figure 13b, c**). These results demonstrated that the IL-18-stimulated macrophages induced apoptosis of endothelial cells, indicating the cause of the defectiveness of blood vessel formation in the MS-K-IL-18 tumors.

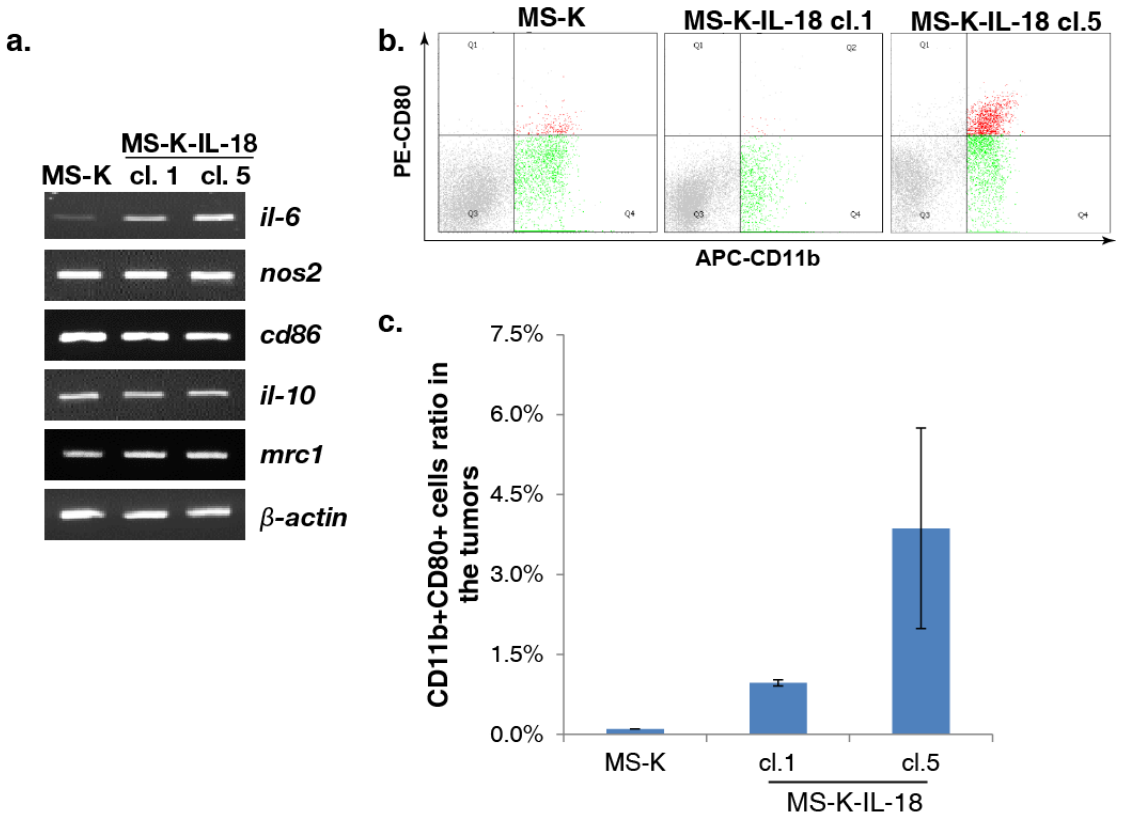

Figure 12. The effect of IL-18 on M1 macrophage polarization.

a. The expression of M1 macrophage marker *il-6*, *nos2* and *cd86*, M2 macrophage marker *il-10*, *mrc1* and *ifn-γ*, and *β-actin* in the sorted CD14+ cells was analyzed by RT-PCR.

b. The number of CD11b and CD80 double positive cells (CD11b+CD80+) was analyzed using flow cytometry.

c. The average percentage of CD11b+CD80+ cells was calculated. * indicates $p < 0.05$ and *** indicates $p < 0.001$.

3.1.7 Summary

In this part, MS-K-IL-18 clones were established to examine the role of IL-18 in tumorigenesis and angiogenesis. The MS-K-IL-18 clones were subcutaneously inoculated into the mice and tumor formation was carried out. Blood vessel formation in these MS-K-IL-18 tumors was less than the parental MS-K tumor and accumulation of M1 macrophages in the MS-K-IL-18 tumor was observed indicated by the M1

macrophage marker *il-6* induction and CD11b+CD80+ cells accumulation. Furthermore, the IL-18-stimulated macrophages induced apoptosis of endothelial cells.

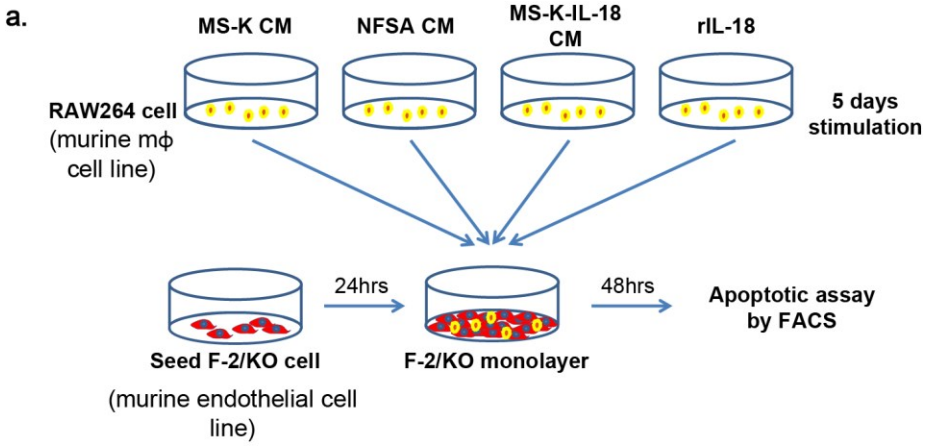

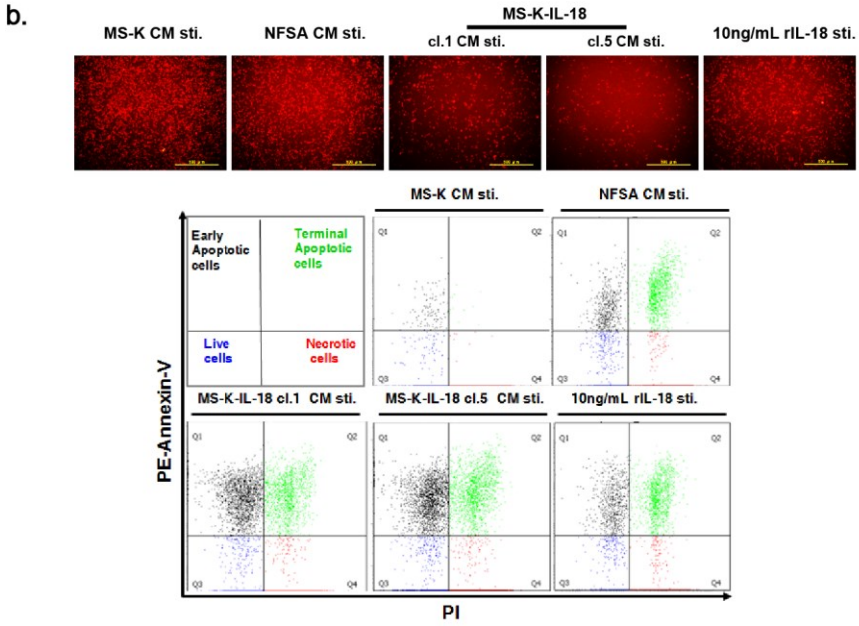

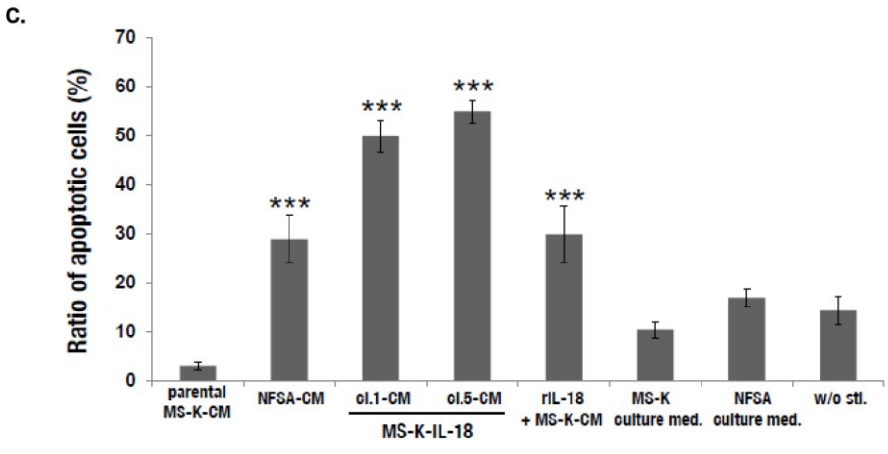

Figure 13. The pro-apoptotic effect of IL-18 stimulated macrophage on endothelial cells.

a. The schematic drawing for the assay of checking the IL-18 effect on endothelial cells exerted by macrophage.

b. The Photographs show the F-2-Kusabira Orange (F-2-KO) cells co-cultured with stimulated RAW cells after 48 hours. The dot plot of the flow cytometry showed the expression of Annexin-V in the co-cultured F2-KO cells was analyzed by FACS Aria II. The corresponding cell condition in each quadrant is illustrated in the first plot.

c. The ratio of apoptotic cells including the early apoptotic cells and the terminal apoptotic cells was calculated (n=3). *** indicates $p < 0.001$.

3.2 The function of CCL11 on tumor formation and angiogenesis

According to the result of IL-18, the IL-18 was responsible for M1 macrophage differentiation, rather than the CD14+ cells accumulation. Therefore, the chemokine ligand family highly expressed in the NFSA cells should be examined. CCL11 showed the greatest diversity in the NFSA cells and MS-K cells. Thus, The CCL11 was overexpressed in the MS-K cells as well. The CCL11 overexpressing clones were intended to use as a resource of CCL11 to check its effect on tumor formation and angiogenesis by some particular immune cells recruitment.

3.2.1 The establishment of CCL11 overexpressing MS-K clones

At first, similarly as IL-18, the CCL11 expression vector using modified pIRES2-ZsGreen1 vector was constructed. The mature CCL11 coding sequence was amplified and cloned into the EF1α promoted-pIRES2-ZsGreen1 vector. Then the vector was transfected into parental MS-K cells. By antibiotic selection and single cell

sorting using flow cytometry, five CCL11 overexpressing MS-K clones (MS-K-CCL11) were selected by fluorescence at first (**Figure 14**).

In the following, RT-PCR and quantitative PCR were performed to examine the *ccl11* expression level. The *ccl11* was highly expressed in the 5 clones, compared to parental MS-K cells and NFSA cells (**Figure 15a**). By quantitative PCR (**Figure 15b**), *ccl11* expression level was reconfirmed. Because the expression level of *ccl11* in the MS-K-CCL11 cl.2 and cl.4 was top two, so these two clones was used in the following assays.

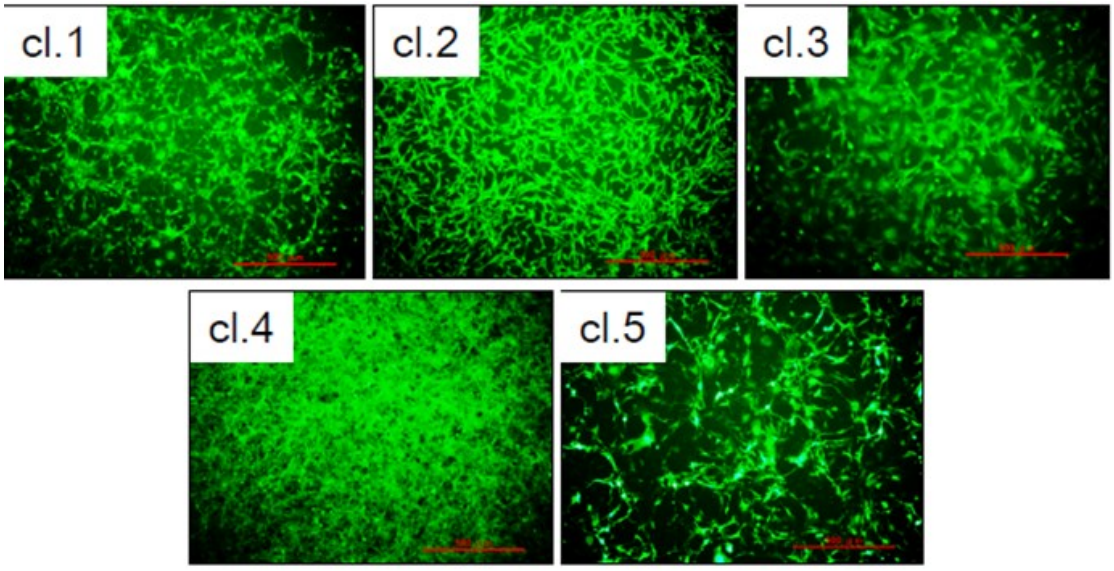

Figure 14. Primary selection of five MS-K-CCL11 clones by fluorescence.

These five clones were simply selected by their strong expression of ZsGreen1.

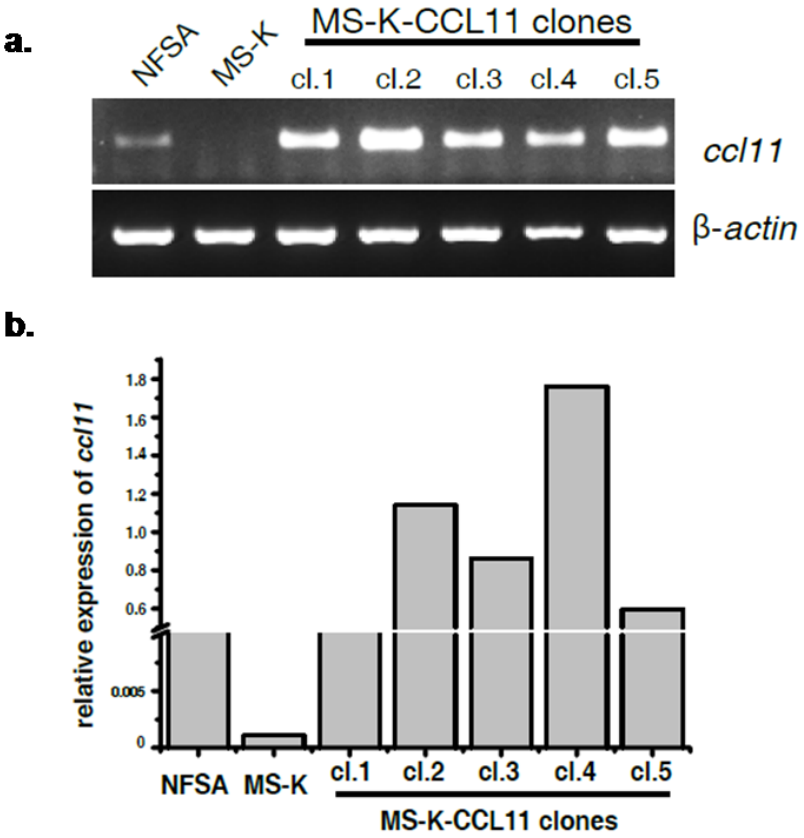

Figure 15. The ccl11 expression in the MS-K-CCL11 clones.

a. The expression of *ccl11* in the MS-K-CCL11 clones was analyzed by RT-PCR.

b. Relative expression of *ccl11* (*ccl11*/*β-actin*) in the MS-K-CCL11 clones was measured by qPCR.

3.2.2 The protein expression in the MS-K-CCL11 clones

Besides mRNA expression level, CCL11 protein expression in MS-K-CCL11 clones was then examined by confocal microscope observation stained with anti-CCL11 antibody (**Figure 16**). The Alexa Fluor 647 labeled anti-rat IgG antibody signal distributed in the cytoplasm of the MS-K-CCL11 cells.

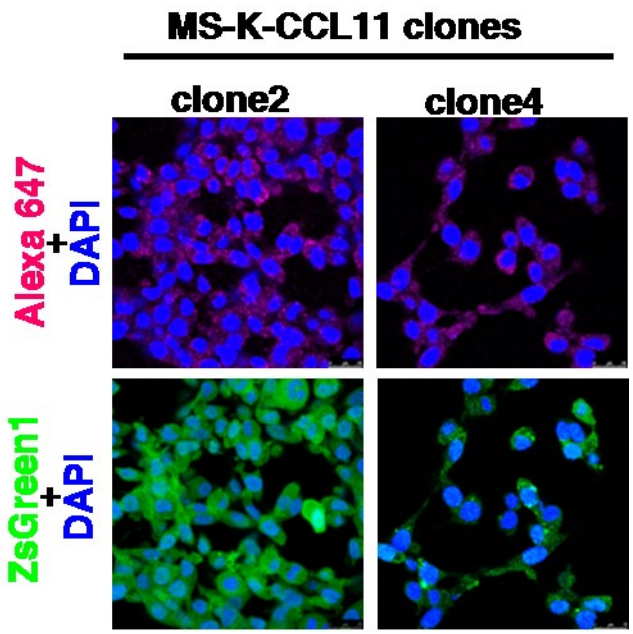

Figure 16. Confocal microscope observation of CCL11 in the MS-K-CCL11 clones. Alexa 647 merged with DAPI indicated the CCL11 distribution, and the ZsGreen1 merged with DAPI indicated the cell shape of the MS-K-CCL11 clones.

Because the CCL11 were designed to be a secreted protein in the MS-K-CCL11 clones, so the CCL11 concentration was quantified in the CM of the MS-K-CCL11 clones compared to parental MS-K, MS-K-mock and NFSA. The results were listed in the **Table 2.**

Table 2 CCL11 quantification in the MS-K-CCL11-CM

Sample name	Concentration of CCL11 in the CM (pg/mL)
Parental MS-K	680.69 ± 10.03
MS-K-mock	641.30 ± 35.48
MS-K-CCL11 cl.2	2075.15 ± 103.62
MS-K-CCL11 cl.4	2053.09 ± 32.61
NFSA	2273.69 ± 23.40

3.2.3 The characterization of MS-K-CCL11 clones *in vitro*

Similarly, the characteristics of the MS-K-CCL11 were examined *in vitro.* Firstly, the cell proliferation assay was carried out to examine the MS-K-CCL11 clone proliferation compared to parental MS-K cells and MS-K-mock cells. The result showed that though NFSA grew slower than MS-K cells, the MS-K-CCL11 clones grew at the same rate as parental MS-K and MS-K-mock clone (**Figure 17**).

The colony formation assay showed that MS-K-CCL11 cl.2 formed significantly less colonies than parental MS-K and MS-K-mock cells (**Figure 18a, b**). These result showed that the MS-K-CCL11 clones were similar with parental MS-K cells.

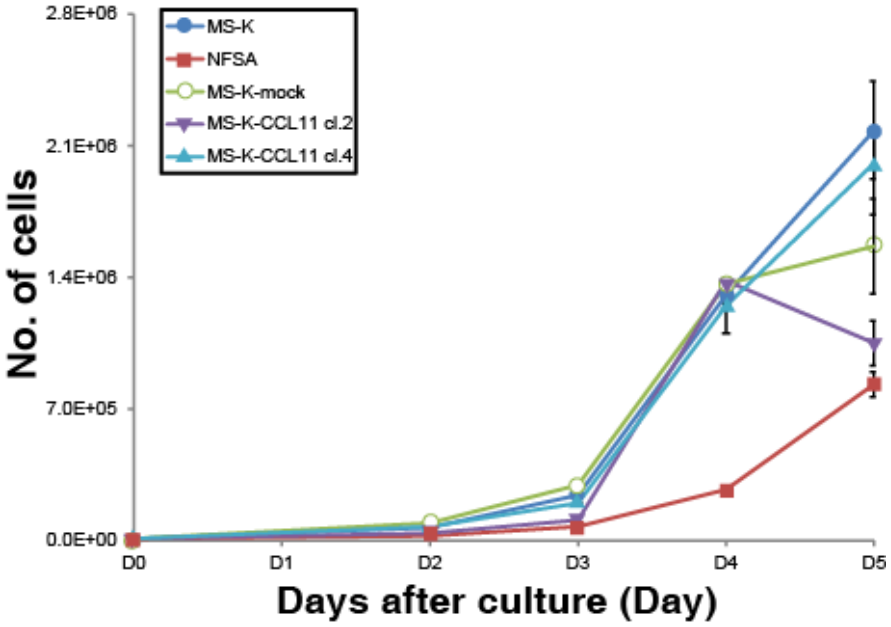

Figure 17. Growth curve of MS-K-CCL11 clones.

The cell number was counted on day 2 to day 5. Data indicated mean ± standard deviation (n = 3).

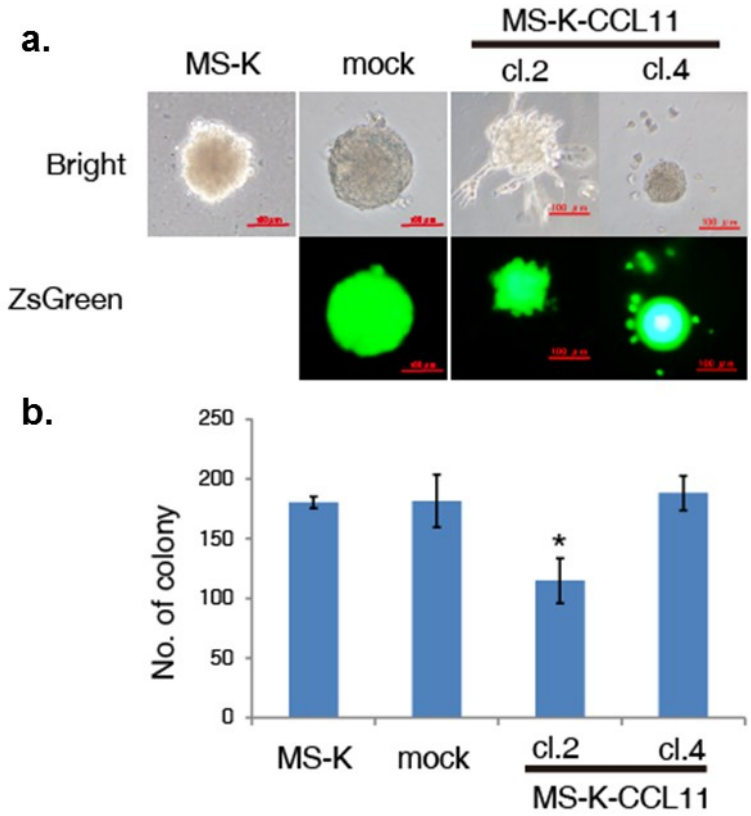

Figure 18. The colony formation analysis for MS-K-IL-18 clones.

a. The photos of the colonies were taken on day 15.

b. The colony numbers were counted on day 15 and the data indicated mean ± standard deviation (n = 4). * indicates $p < 0.05$.

3.2.4 The effect of CCL11 on granulocyte differentiation

The MS-K-CCL11 clones and parental MS-K cells were subcutaneously inoculated into mice to evaluate the function of CCL11 in tumors. Surprisingly, when parental MS-K cells formed big tumors, both MS-K-CCL11 clones did not form any tumors for 30 days after inoculation. And by colony formation assay, both MS-K-CCL11 clones formed colonies *in vitro.* Thus I wondered if the MS-K- CCL11 tumor cells were damaged or killed by some immune cells recruited by the excess CCL11 secreted by MS-K-CCL11 cell itself *in vivo*.

Because CCL11 were firstly characterized as a chemoattractant of eosinophils, to test the hypothesis, the effect of the MS-K-CCL11-CM on granulocyte differentiation was firstly analyzed. The bone marrow cells were cultured with the MS-K-CCL11-CM and rG-CSF. After 7 days of culture, the MS-K-CCL11-CM induced macrophage, neutrophil, and eosinophil differentiation (**Figure 19**). The eosinophil expression markers, *siglec-f* and *ccr3* were specifically induced by MS-K-CCL11-CM, which indicated that the eosinophils were induced by the CCL11 which was produced by MS-K-CCL11 cells.

Furthermore, the effects of MS-K-CCL11-CM and recombinant CCL11 on differentiation of the eosinophil was analyzed by analyzing the Siglec-F+Gr-1+ cell ratio in the differentiated BM cells by flow cytometry (**Figure 20**). The Siglec-F+Gr-1+ cells were dose-dependently induced by the MS-K-CCL11-CM or rCCL11, which suggested that the differentiation of the BM cells into eosinophils was dependent upon CCL11 to some extent. Thus, the high dose of CCL11 produced by MS-K-CCL11 cells must have strongly induced the eosinophil differentiation in the MS-K-CCL11-transplanted mice.

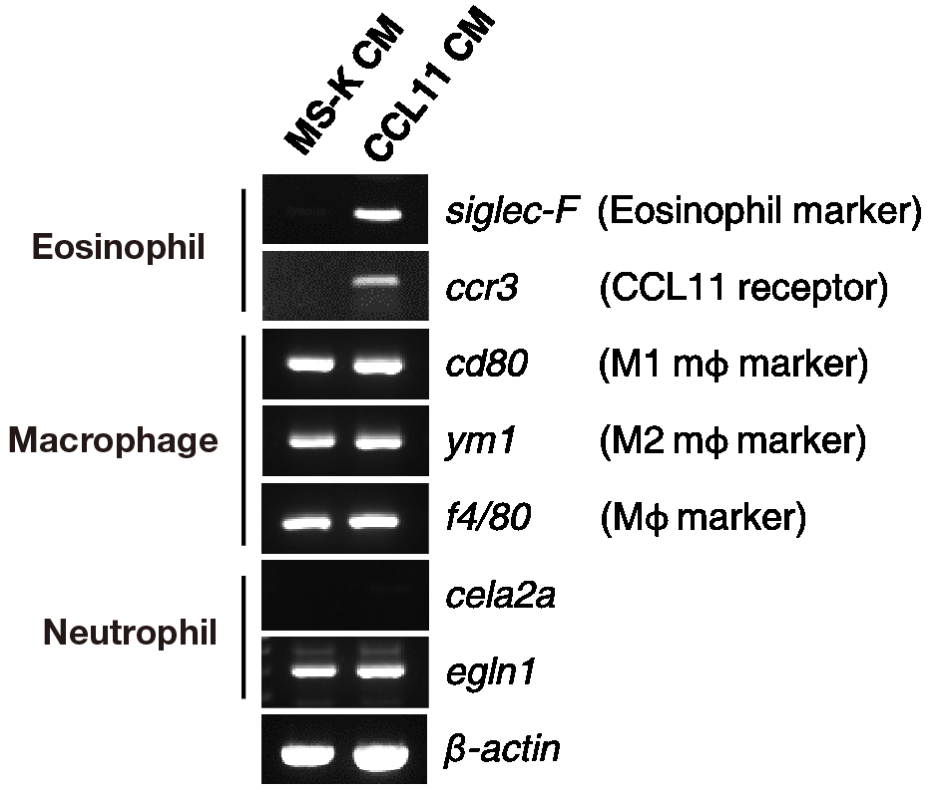

Figure 19. CCL11 induced the expression of *siglec-f* and *ccr3* in the bone marrow cells.

The BM cells were stimulated with G-CSF and MS-K-CCL11-CM or MS-K-CM for 7 days. Then, the expression of granulocyte and macrophage specific markers was analyzed by RT-PCR.

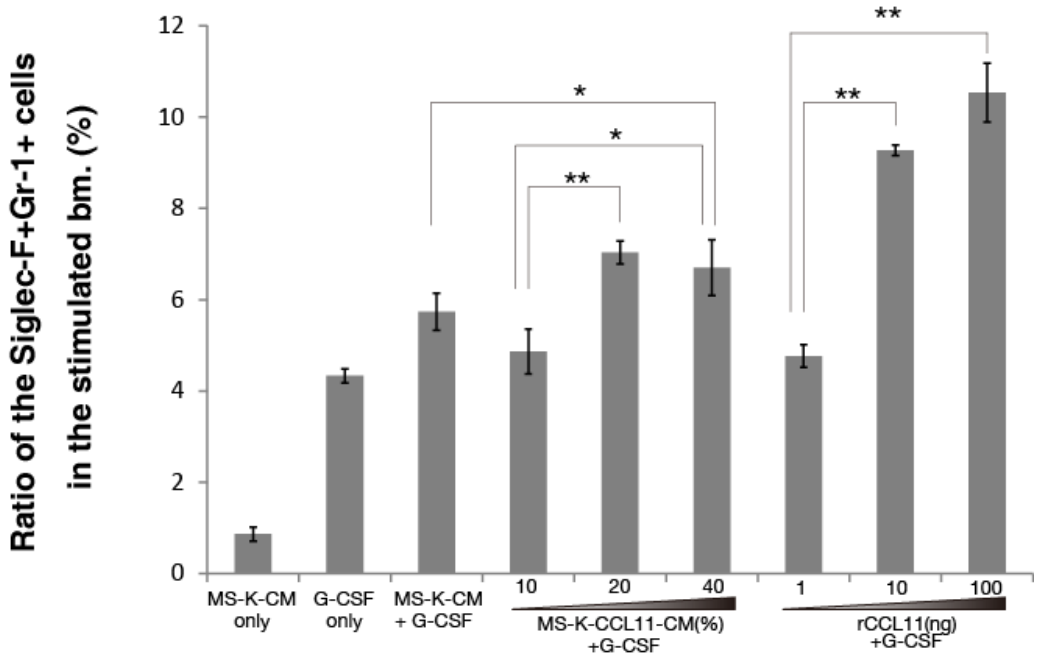

Figure 20. CCL11 induced the Siglec-F+Gr-1+ cells in the bone marrow.

The BM cells were incubated with the MS-K-CCL11-CM or rCCL11 with G-CSF in semi-solid medium for 7 days. Then, the ratio of the Siglec-F+Gr-1+ cells was analyzed as eosinophils by flow cytometry (n = 3). A significant difference was indicated by *, $p < 0.05$ and **, $p < 0.01$.

3.2.5 The effect of CCL11 on granulocyte migration

In the following, the effect of CCL11 on eosinophil recruitment was analyzed. The BM cells were firstly stimulated with MS-K-CCL11-CM to induce the eosinophil differentiation, and then the stimulated BM cells were used as the source of eosinophils for a transwell migration assay. The purple area indicated the transmembrane cells in the lower side of the membrane which was recruited from the upper chamber by the CCL11 in the MS-K-CCL11-CM (**Figure 21a**). The results indicated that CCL11 which was enriched in the MS-K-CCL11-CM strongly recruited the differentiated eosinophils (**Figure 21b**).

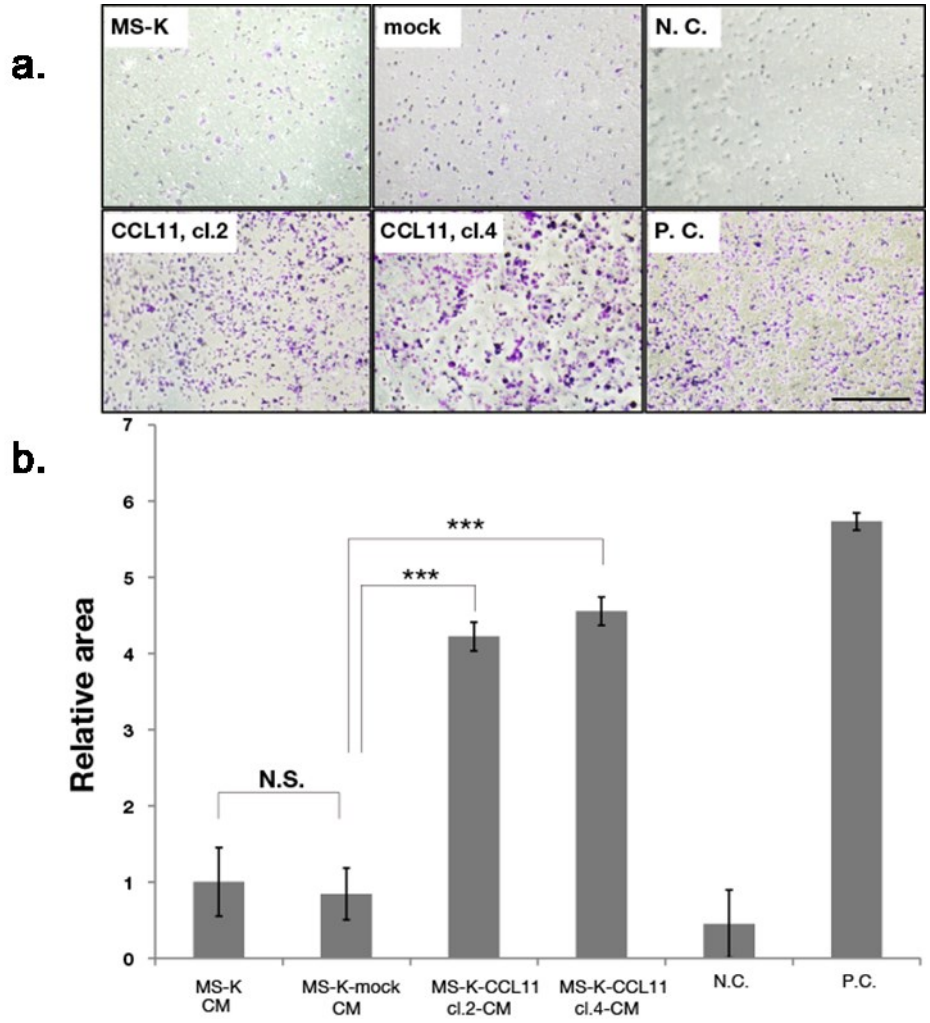

Figure 21. CCL11 induced the migration of eosinophils.

The function of CCL11 on eosinophil recruitment was evaluated with a transwell migration assay. The MS-K-CCL11-stimulated BM cells were seeded on the upper chamber of the filters.

a. The cells that migrated to the underside of the filters after 90 minutes of culture were fixed and stained with crystal violet. The scale bar represents 500 μm. The photographs indicate the migrated cells that were stained with the crystal violet.

b. The histogram shows the quantification of the area covered by the migrated BM cells. The area covered by the migrated cells with the MS-K-CM was set to 1. Each bar indicates the relative area (average ± standard deviation) of three independent transwells (n = 3). A significant difference was indicated by ***, $p < 0.001$.

3.2.6 The eosinophil infiltration in the NFSA tumors

I next intended to examine if eosinophils were accumulated in the NFSA tumors, in order to verify the hypothesis. The day 18 NFSA tumor paraffin sections were used to perform the immunohistochemical staining using anti-Siglec-F antibody. The result showed that the Siglec-F+ eosinophils distributed in the NFSA tumors in an agminated manner (**Figure 22a**).

In further, the time course of Siglec-F+Gr-1+ cells infiltration in the NFSA tumors was analyzed. The NFSA cells were subcutaneously injected into the mice, and on day9, day12 and day18, the tumors were excised and the single cells were prepared to perform the analysis using flow cytometry (**Figure 22b**). The result showed that the ratio of the Siglec-F+Gr-1+ cells increased along with the tumor growth. It was convinced that the eosinophil did infiltrate into NFSA tumors and its population increased with the tumor growth.

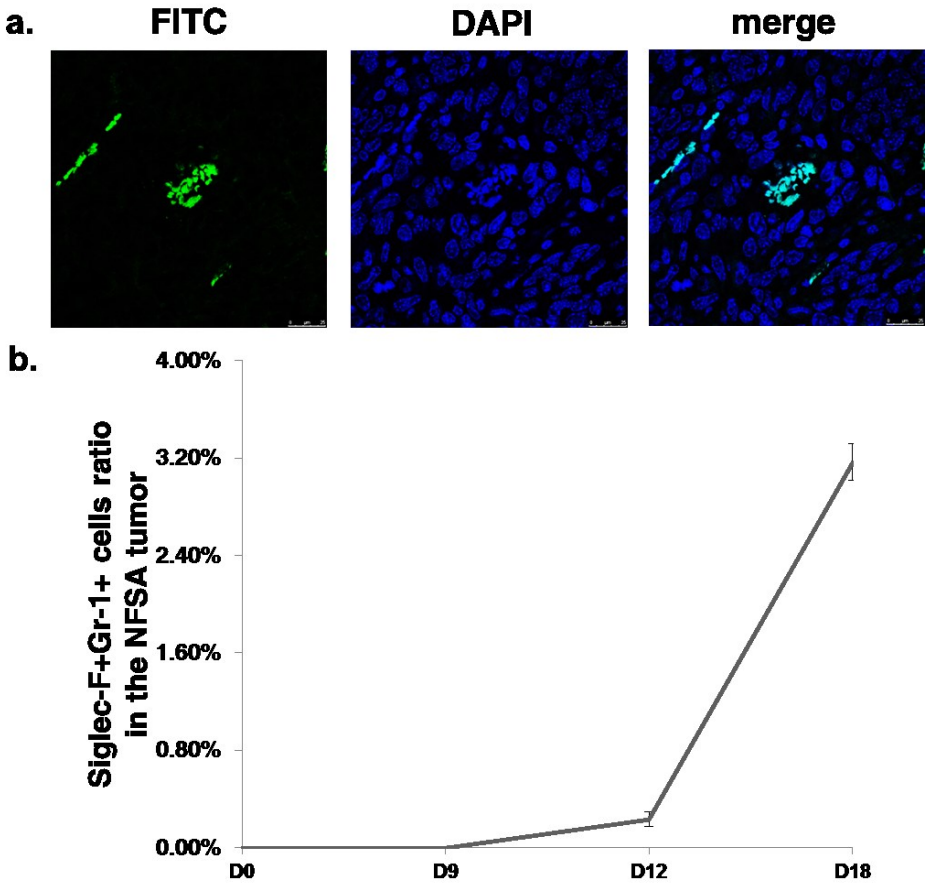

Figure 22. The infiltration of eosinophils in the NFSA tumors.

a. The eosinophils were stained with anti-Siglec-F antibody as 1st antibody, and FITC labeled anti-rat IgG antibody as 2nd antibody. Bar is 25 μm.

b. The NFSA tumor infiltrated eosinophils ratios were analyzed on day 9, day 12 and day 18. Data indicated mean ± standard deviation (n = 3).

3.2.7 The effect of the CCL11 induced-eosinophils on tumor and endothelial cells

I already examined the CCL11 function on the eosinophil differentiation and migration, most of all, whether the recruited eosinophils could have negative effects on tumor cells growth should be tested in the following. The cytotoxicity of CCL11 induced-eosinophils on tumor cells and endothelial cell growth were examined using a co-culture system *in vitro*. The BM cells were stimulated with MS-K-CCL11-CM or MS-K-CM that were overlaid on a monolayer of fluorescent-labeled MS-K-GFP cells, NFSA-GFP cells or F-2-Kusabira Orange cells at various ratios. After 48 hours, the number of living the MS-K-GFP, NFSA-GFP, or F-2-Kusabira Orange cells were counted by FACS. Many monolayer cells were killed due to the increase in effector cell numbers (**Figure 23a, c, e**). Notably, the cytotoxicity of the BM cells that were stimulated with MS-K-CCL11-CM damaged both the tumor and endothelial cells more significantly than the BM cells that were stimulated with MS-K-CM (**Figure 23b, d, f**). These results demonstrated that CCL11 stimulated BM cells could damage both tumor and endothelial cells. Therefore, these results indicated that the infiltrated eosinophils in the tumor would not only block tumor formation but would also reverse the angiogenesis.

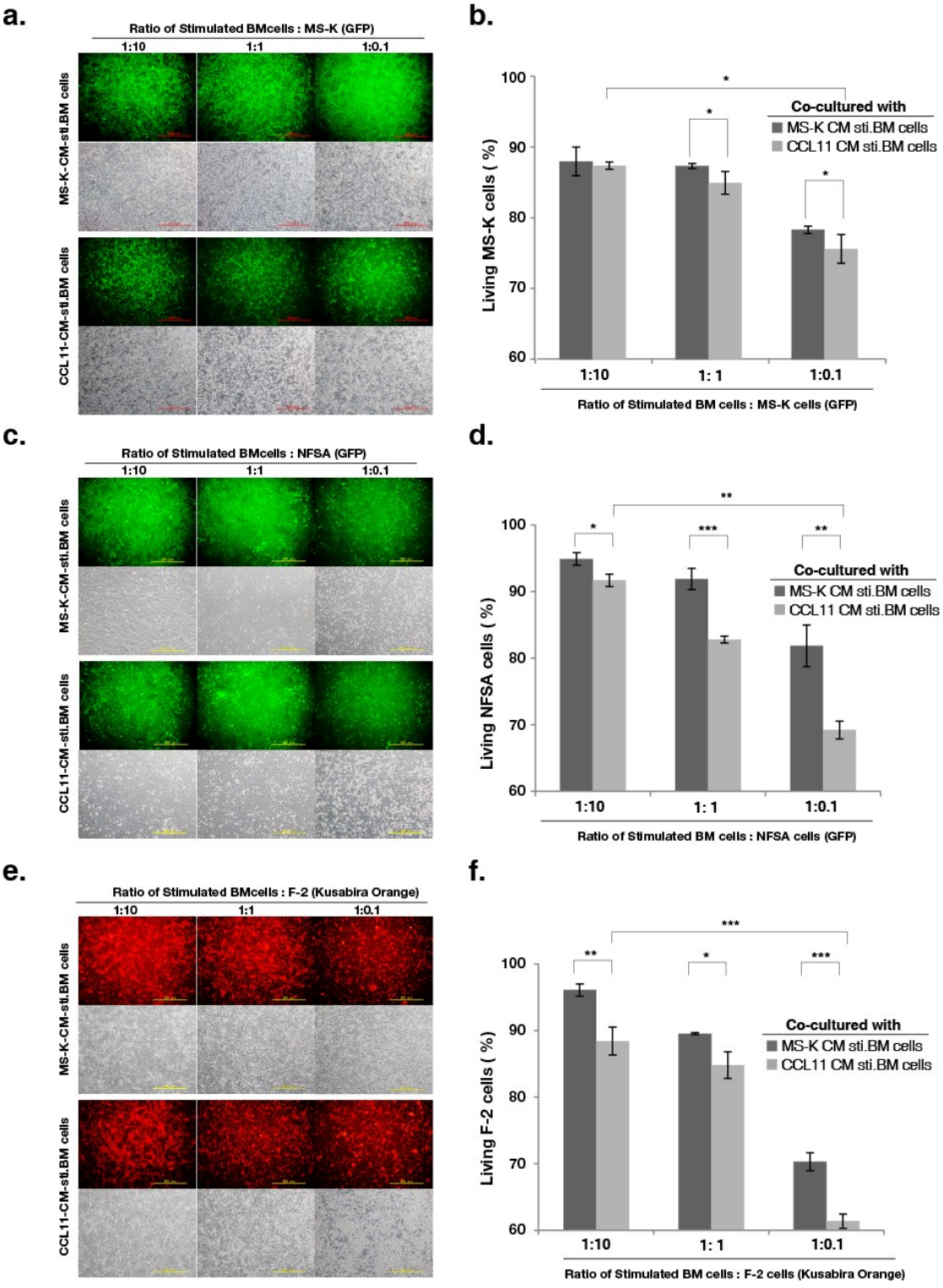

Figure 23. The effect of CCL11 induced eosinophils on tumor cells and the endothelial cell *in vitro*.

The BM cells were stimulated by MS-K-CCL11-CM or MS-K-CM with G-CSF for 7 days. Then, the stimulated BM cells were overlaid on the monolayer of MS-K-EGFP (a),

NFSA-EGFP (c) or F-2-Kusabira Orange cells (e) at the various ratios described in the figure. Photographs were taken after 48 hours. The upper photographs were fluorescent, and the lower was phase contrast. The bar represents 500 μm. The histogram (b, d and f) shows the number of living cells counted by FACS. Significant differences are shown by *, $p < 0.05$; **, $p < 0.01$; ***, $p < 0.001$.

3.2.8 The effect of specific CCR3 antagonist on NFSA tumor

The preceding research demonstrated the excess CCL11 affected the MS-K tumor growth and angiogenesis. On the other hand, in case of blocking the CCL11 in the NFSA tumor which highly expressed CCL11, its effects on tumor growth and angiogenesis should also be examined.

Therefore, the CCR3 specific antagonist SB 328437 was applied to inhibit the activity of CCR3. As the result, it would suppress the induction of eosinophils via inhibition of CCL11 activity. The assay was carried out by subcutaneously injection of NFSA tumor cells firstly, followed by intraperitoneal injection of the SB 328437 for 2 weeks. Then the tumors were excised and angiogenesis was determined by immunohistochemical staining. The eosinophils infiltration was analyzed by flow cytometry.

On day 18, tumors were excised from mice and the weight of tumors was measured. The average tumor weight was increased but not significant (**Figure 24a**). Moreover, the tumor showed blood vessels were enriched in the 5 mg/kg administration group than the 1 mg/kg group and vehicle group. The dotted line indicated recovered angiogenesis area (**Figure 24b**).

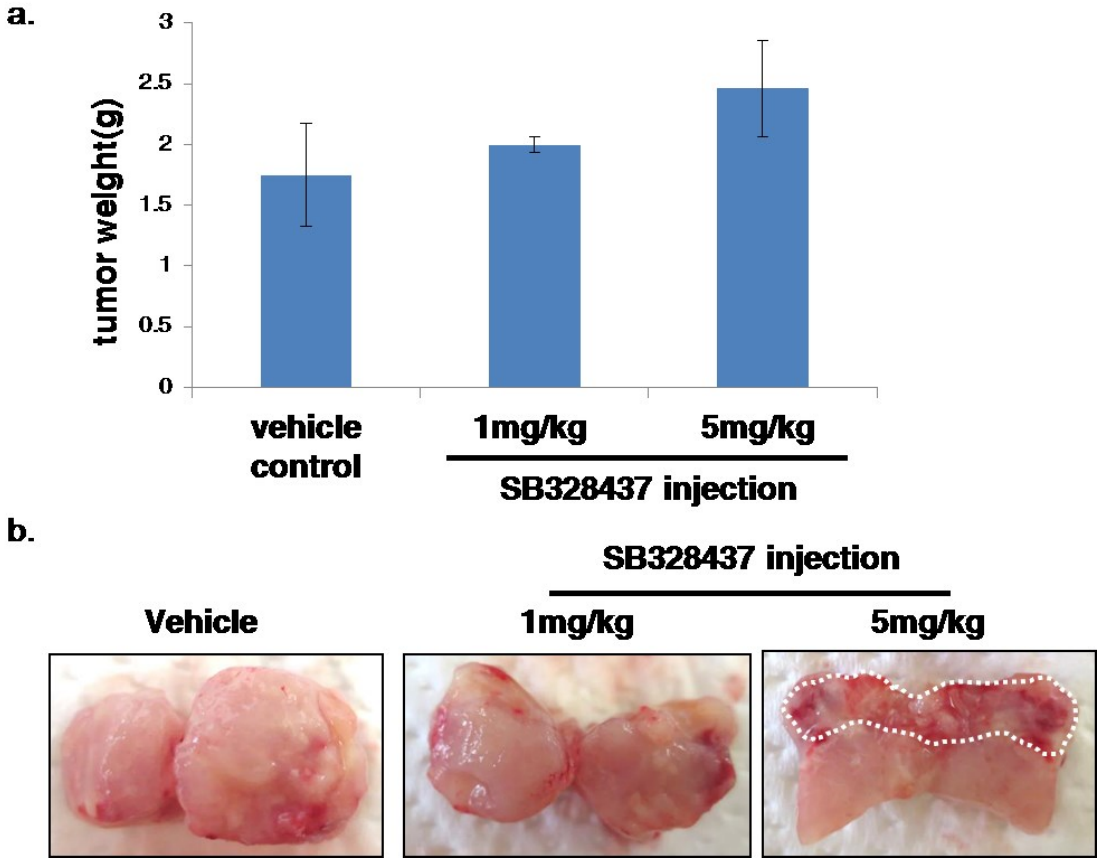

Figure 24. The effect of CCR3 antagonist on the NFSA tumor growth.

a. The tumor weight were measured after excision Data indicated mean ± standard deviation (n = 3).

b. The NFSA tumors were cut into halves, and the photos were taken. Dot plot indicated the enriched blood vessels area in the 5 mg/kg injection group.

In the following, the infiltration immune cells ratio was checked by APC-CD14 and PE-Gr-1 double staining to analyze the granulocyte infiltration **(Figure 25a),** and PE-Gr-1 and APC-Siglec-F double staining to analyze the eosinophil infiltration (**Figure 25b**). High dose of CCR3 antagonist (5 mg/kg) could effectively block the granulocyte infiltration (vehicle group: 18.8 % ± 1.1 % vs. 5 mg/kg inhibitor group: 15.0 ± 0.8%) and eosinophil infiltration (vehicle group: 3.2 % ± 0.2 % vs. 5 mg/kg inhibitor group: 2.6 % ± 0.1 %).

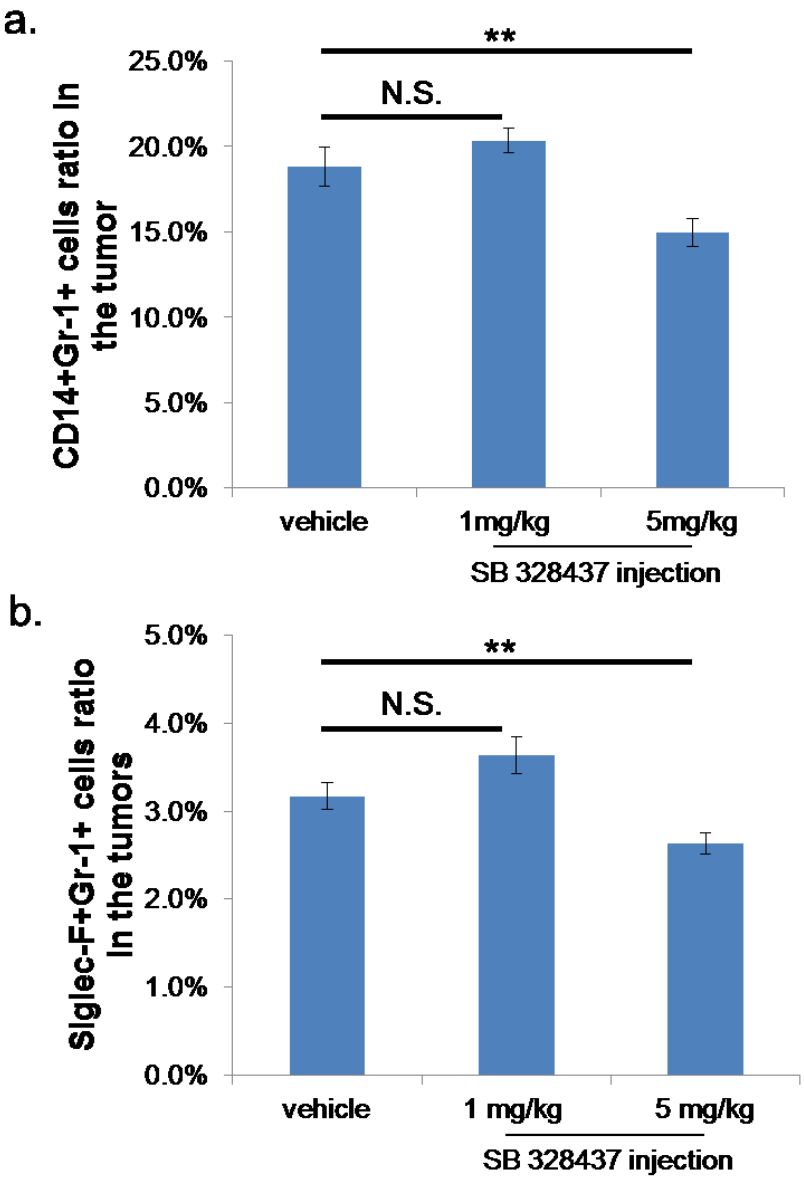

Figure 25. The effect of CCR3 antagonist on granulocyte and eosinophil infiltration.

a. The CD14+Gr-1+ cells ratio was analyzed by flow cytometry. Data indicated mean ± standard deviation (n = 3). Significant differences are shown by **, $p < 0.01$.

b. The Siglec-F+Gr-1+ cells ratio was analyzed by flow cytometry. Data indicated mean ± standard deviation (n = 3). Significant differences are shown by **, $p < 0.01$.

Besides examining the immune cells infiltration, the angiogenesis status was also checked by immunohistochemical staining using the anti-CD31 antibody (**Figure 26**). In the vehicle group and 1 mg/kg group, the blood vessel status was same as the

NFSA tumor that no blood vessel can be detected. However, in the 5 mg/kg SB 328437 group, the blood vessels were obviously observed.

These results demonstrated that the administration of CCR3 antagonist led to the blockade of eosinophils infiltration and the restoration of blood vessel formation, which indicated that the eosinophils play a vital role in damaging the blood vessels in the NFSA tumors.

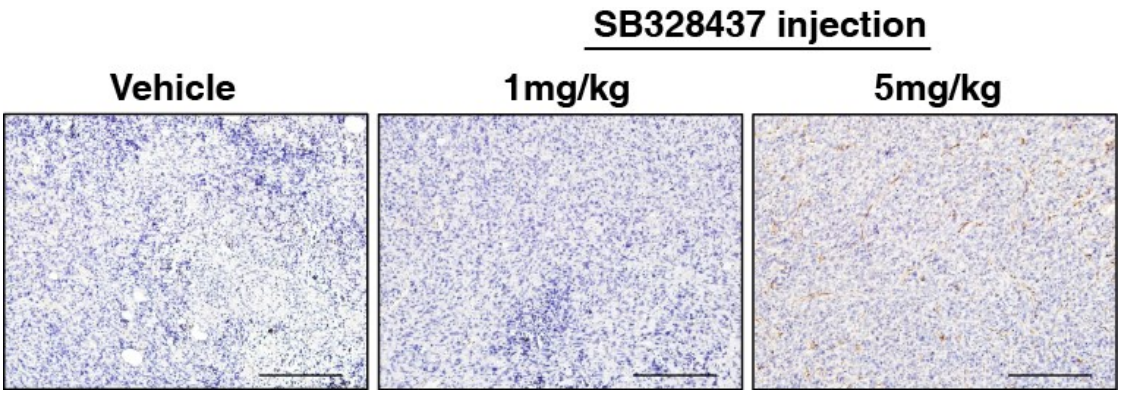

Figure 26. The effect of CCR3 antagonist on blood vessel formation in the NFSA tumors.

The blood vessels were checked by the anti-CD31 antibody, and after histochemical staining, the tumor slides were counterstained by hematoxylin. The brown signals indicated the blood vessels.

3.2.9 Summary

In this part, I mainly focused on the CCL11 effect on the MS-K tumor growth, elucidated its function on inducing the eosinophil differentiation and migration and confirmed the eosinophil tumoricidal effects on tumor cells and endothelial cells. Moreover, by CCL11 receptor CCR3 specific antagonist, it was demonstrated that the blood vessel formation was restored in the NFSA tumors by the diminished ratio of eosinophils blocked by the CCR3 antagonist SB 328437. These data explained the reason for the diminished tumor formation by the MS-K-CCL11 cells: the

overexpressed CCL11 by the MS-K-CCL11 cells induced eosinophils in the mice. Then the CCL11 attracted eosinophils to the MS-K-CCL11 tumors, and the attracted eosinophils damaged the MS-K-CCL11 itself as well as the endothelial cells. Therefore, the transplanted MS-K-CCL11 cells could not form tumors.

4. Discussion

4.1 Characteristics of IL-18-overexpressing MS-K

There was significant difference in blood vessel formation between MS-K tumor and NFSA tumor [34], and the expression of the *il-18* was only detected in the NFSA by RT-PCR. Thus, I tried to overexpress the *il-18* in the MS-K cell to analyze the role of the *il-18* in tumorigenesis and angiogenesis in MS-K tumor. The IL-18-overexpressing MS-K cells revealed less proliferation and colony formation ability compared to the parental MS-K cells (**Figure 7, 8**). These results indicated that IL-18 might affect the cell proliferation. Furthermore, the expression of the IL-18 receptor 1 was upregulated in the IL-18-overexpressing MS-K clones (**Figure 5a**). It was reported that IL-18 may inhibit the proliferation of chondrocyte [43], and IL-18 could stimulate a positive feedback loop through the IL-18 receptor to increase its own IL-18-expression and production [44]. Therefore, that may be the cause of less proliferative and smaller colony formation ability of the IL-18-overexpressing MS-K than the parental MS-K.

Nevertheless, the MS-K-IL-18 tumors weight was not reduced significantly. Excess IL-18 resulted in the blood vessel formation inhibition, however, the VEGF-A expression in the MS-K-IL18 clones was not affected compared with parental MS-K cell (**Figure 5a**). Thus, it is possible that the IL-18 did not play the central and vital role in manipulating the MS-K tumor growth. Similar to NFSA tumor, MS-K-IL-18 tumor may grow in a VEGF-A-dependent but angiogenesis-independent manner [45].

4.2 Effect of IL-18 on polarization M1 macrophages in the MS-K-IL-18 tumor

Tumor–associated macrophages (TAM) are a major type of infiltrating immune cells and are critical regulators of the balance between inflammation and cancer [46]. Monocytes in circulation infiltrate into the tumor niche and differentiate into two

functionally opposite types of macrophages: classically activated macrophages (M1 type) and alternatively activated macrophages (M2 type). The differentiation is controlled by various tumor-derived factors. Briefly, M1 type macrophages have Th1-oriented immunostimulatory properties, such as production of cytotoxic and anti-tumor factors [47]. M2 type macrophages suppress Th1 adaptive immunity, promote wound healing, induce angiogenesis, and remodel the extracellular matrix [48]. These polarized macrophages are distinguished by different receptor expression and inflammatory factor production [49]. Expression of *il-6,* which was the marker of M1 macrophage, was increased in the CD14+ cells derived from the MS-K-IL-18 tumors (**Figure 12a**). Moreover, the ratio of M1 macrophage represented by CD11b+CD80+ cells was increased in the MS-K-IL-18 clones (**Figure 12b, c**). These findings indicated that IL-18 induced M1 type macrophages. IFN-γ is also responsible for M1 type macrophage polarization [50]. IL-18 was initially characterized as a potent inducer of IFN-γ [51]. However, the expression of the *ifn-γ* gene was reduced in the CD14+ cells derived from MS-K-IL-18 tumors (**Figure 12a**). These data suggest that IL-18 induced the polarization of M1 macrophages in an *IFN-γ*-independent manner both *in vivo* and *in vitro.*

4.3 IL-18-stimulated macrophages caused apoptosis in endothelial cells

Besides, inducible nitric oxide synthase (iNOS/Nos2) has been directly implicated in macrophage-mediated tumoricidal activity [52]. The iNOS expressing monocytes infiltrate into CT26/IκB-αSR tumors are associated with higher levels of tumor cell depopulation [53]. *In vitro* studies have shown IL-18 damaged the endothelial cells by induction of Nos2 and production of NO [34]. However, the expression level of *nos2* in CD14+ cells derived from MS-K-IL-18 tumors was similar to control CD14+ cells (**Figure 12a**). This result indicated the Nos2/NO system was not responsible for the failure of blood vessel formation in the MS-K tumor microenvironment.

Amongst the list of factors induced in M1 type macrophages [49], IL-6 is reported to inhibit endothelial cell proliferation and VEGF-induced angiogenesis in a rabbit corneal assay [54]. Increased levels of IL-6 protein are detected in the supernatants of chondrocytes stimulated with IL-18 [43]. Our results showed only IL-6 expression was upregulated in the CD14+ cells derived from MS-K-IL-18 tumors (**Figure 12a**).The cell junction in the MS-K-IL-18 cl.5 tumor core was damaged, which was indicated by the pale counterstaining with hematoxylin (**Figure 10a**). Thus, I tested the effect of IL-18-stimulated RAW264 cells on survival of endothelial cell line. The MS-K-IL-18-CM or rIL-18 stimulated macrophages damaged the endothelial cells by accelerating their apoptosis (**Figure 13**). Therefore, the blood vessel formation in the MS-K-IL-18 tumors must be blocked by the polarized M1 macrophages by excess IL-18.

4.4 Pro-inflammatory genes in the CD14+Gr-1+ cells

It is known that macrophages that infiltrate tumors play critical roles in modulating tumor growth and angiogenesis [16]. On the other hand, the role of granulocytes that infiltrate tumors had not been elucidated completely. In the pre-research, I observed a significant difference in the accumulation of CD14+Gr-1+ cells into NFSA tumors compared with MS-K tumors (**Figure 2**); therefore, I believe that the significant accumulation of the CD14+Gr-1+ cells was a reason for the severe necrosis observed in the NFSA tumors. The expression gene analysis of the CD14+Gr-1+ cells that infiltrated the NFSA tumors revealed high expression levels of several pro-inflammatory genes (**Figure 2b**). Nos2 was reported to relate to M1 macrophage activation [16] and production of nitric oxide; subsequently, it was shown to be involved in the pathogenesis of inflammation [55]. TNF-α exhibited anti-tumor activity in both *in vitro* and *in vivo* experiments [56-58]. Cathelicidin antimicrobial peptide (CAMP) is an important effector of the innate immune system, with direct

anti-bacterial activity. CAMP expressed from myeloid cells promotes lung tumor growth by further recruitment of inflammatory cells [59]. CELE2A was expressed not only by neutrophils and eosinophils [60] but also by some tumor cells. Increased CELE2A levels were shown to be associated with recurrence and death in breast cancer patients [61]. Ectopic expression of Egln1 [62], Egln2 [63] and Egln3 [64] suppressed the accumulation of hypoxia-inducible factor α (HIF-1α). Furthermore, Egln2 inhibited tumor growth by increased necrosis and decreased micro-vessel density [63]. Therefore, high expression of these pro-inflammatory genes in the CD14+Gr-1+ cells implies that the necrosis in the core of the NFSA tumors was caused by these cytotoxic and anti-tumoral factors.

4.5 Effect of CCL11 on growth of the tumor

The effect of CCL11 on CD14+Gr-1+ cell recruitment *in vivo* was analyzed. For this purpose, the overexpression of CCL11 was done in the MS-K cells to simply mimic CCL11 expression in the NFSA cells. The CCL11 expression level in the MS-K-CCL11 was very high compared with the parental NFSA and MS-K cells (**Figure 15, Table 2**). Surprisingly, the MS-K-CCL11 clones did not form a tumor after subcutaneous inoculation in the abdomen. As there was no significant difference in the growth and colony formation abilities between the MS-K-CCL11 and MS-K cells (**Figure 17, 18**), I think that the MS-K-CCL11 cells were damaged by the immune cells in the host mice.

4.6 Effect of CCL11 on differentiation of the granulocyte

To elucidate the reasons for the diminished tumor formation from the MS-K-CCL11 cells, the effect of CCL11 on granulocyte differentiation was analyzed. Human CCL11 was found to be involved in the differentiation of human CD34+ progenitors into eosinophils, and this eosinophil differentiation occurred in an IL-3-,

IL-5-, and GM-CSF-independent manner [65]. Here, I demonstrated that MS-K-CCL11-CM, as well as recombinant CCL11, induced the BM cells to differentiate into eosinophils in the presence of G-CSF (**Figure 19, 20**). The CCR3 [66] and Siglec-F [67] expression levels were induced in the BM cells that were stimulated only by MS-K-CCL11-CM but not by MS-K-CM (**Figure 19**), which indicated that the eosinophil differentiation in the NFSA tumors was induced by the CCL11 stimulation. It was reported that eosinophil differentiation is induced by a series of factors, including IL-3 and GM-CSF for the early stage differentiation [68] and IL-5 for terminal maturation [69]. IL-3, G-CSF, GM-CSF, and IL-5 were not expressed in the MS-K cells, although some eosinophils were induced by the parental MS-K-CM (**Figure 19**). This suggested that some other factor(s) in the MS-K-CM were also responsible for eosinophil differentiation. Further analysis of the DNA microarray data indicates that X-box binding protein 1 (Xbp1) expression levels were high in the MS-K cells (**Supplemental table 2**). XBP1 is indispensable for eosinophil production; therefore, ablation of Xbp1 results in a complete and cell-intrinsic loss of both mature eosinophils and their progenitors [70]. Thus, although the MS-K did not produce CCL11, the basic XBP1 in the MS-K-CM may sustain eosinophil maturation.

4.7 Effect of CCL11 on recruitment of the eosinophil

On the other hand, it was previously reported that CCL11 is able to induce the migration of human CCR3-positive endothelial cells and promote the formation of blood vessels *in vivo* [71]. Moreover, eosinophil accumulation within the necrotic areas of solid tumors represented a physiologic response [72] that facilitated tumor growth by remodeling the tumor microenvironment. Ectopic CCL11 expression resulted in increased inflammation, microvascular density, and blood clotting in B16 melanoma cell tumors [73]. The migration assay also demonstrated that the overexpressed CCL11 by the MS-K-CCL11 cells effectively recruited eosinophils

(**Figure 21**).

4.8 Effect of CCR3 antagonist on NFSA tumor growth

Though the CCL11 can induce and recruit the eosinophils into the tumor and these eosinophils would damage the endothelial cells and tumor cells *in vitro*, the *in vivo* mechanism were not fully understood. I tried to knock out the CCL11 in the NFSA cells by CRISPR-Cas9 system [74]. I designed the specific gRNA targets for CCL11; however, the bottleneck problem was to transfect the NFSA cells. Alternatively, I performed the *in vivo* administration assay to elucidate the function of CCL11 from another perspective. I chose the CCL11 receptor CCR3 specific antagonist SB 328 437 to block the CCL11 signals pathway. The result indicated that the high dose of SB 328437 (5mg/kg mouse body weight) could effectively block the eosinophils infiltration and as a consequence, the blood vessel in the NFSA tumors was restored. These data indicate a new target for modulation of blood vessel formation in the tumors, though the eosinophilia were also a pathological problem [75] .

4.9 Conclusion

In conclusion, IL-18 and CCL11 both present tumoricidal effects on MS-K tumors: Excess IL-18 produced by MS-K-IL-18 induced M1 macrophages and inhibited blood vessel formation by pro-apoptotic capability exerted by macrophage on endothelial cells. On the other hand, Tumor infiltrated eosinophils, which were induced and attracted by excess CCL11 produced by MS-K-CCL11 cells, would damage not only the endothelial cells but also the MS-K-CCL11 cells and would block MS-K tumor formation.

These results indicate IL-18 could be a therapeutic target to control M1 type macrophages and inflammation and elucidate a critical role for CCL11-CCR3 signal on eosinophils in the tumor growth and the inflammatory process.

Reference

1. Quail, D.F. and J.A. Joyce, Microenvironmental regulation of tumor progression and metastasis. Nature medicine, 2013. **19**(11):1423-1437.
2. Folkman, J., Tumor angiogenesis: therapeutic implications. New England Journal of Medicine, 1971(285):1182-6.
3. Dvorak, H.F., Vascular permeability factor/vascular endothelial growth factor: a critical cytokine in tumor angiogenesis and a potential target for diagnosis and therapy. Journal of clinical oncology, 2002. **20**(21):4368-4380.
4. Yonekura, H., S. Sakurai, X. Liu, et al., Placenta growth factor and vascular endothelial growth factor B and C expression in microvascular endothelial cells and pericytes implication in autocrine and paracrine regulation of angiogenesis. Journal of Biological Chemistry, 1999. **274**(49):35172-35178.
5. Rissanen, T.T., J.E. Markkanen, M. Gruchala, et al., VEGF-D is the strongest angiogenic and lymphangiogenic effector among VEGFs delivered into skeletal muscle via adenoviruses. Circulation research, 2003. **92**(10):1098-1106.
6. Ding, W., T.R. Knox, R.C. Tschumper, et al., Platelet-derived growth factor (PDGF)–PDGF receptor interaction activates bone marrow–derived mesenchymal stromal cells derived from chronic lymphocytic leukemia: implications for an angiogenic switch. Blood, 2010. **116**(16):2984-2993.
7. Presta, M., P. Dell'Era, S. Mitola, et al., Fibroblast growth factor/fibroblast growth factor receptor system in angiogenesis. Cytokine & growth factor reviews, 2005. **16**(2):159-178.
8. Tait, C.R. and P.F. Jones, Angiopoietins in tumours: the angiogenic switch. The Journal of pathology, 2004. **204**(1):1-10.
9. You, W.-K. and D.M. McDonald, The hepatocyte growth factor/c-Met signaling pathway as a therapeutic target to inhibit angiogenesis. BMB reports, 2008. **41**(12):833.

10. Carmi, Y., E. Voronov, S. Dotan, et al., The role of macrophage-derived IL-1 in induction and maintenance of angiogenesis. The Journal of Immunology, 2009. **183**(7):4705-4714.
11. Wang, Z., J.-Q. Liu, Z. Liu, et al., Tumor-derived IL-35 promotes tumor growth by enhancing myeloid cell accumulation and angiogenesis. The Journal of Immunology, 2013. **190**(5):2415-2423.
12. Ramesh, R., A.M. Mhashilkar, F. Tanaka, et al., Melanoma differentiation-associated gene 7/interleukin (IL)-24 is a novel ligand that regulates angiogenesis via the IL-22 receptor. Cancer research, 2003. **63**(16):5105-5113.
13. Volpert, O.V., T. Fong, A.E. Koch, et al., Inhibition of angiogenesis by interleukin 4. The Journal of experimental medicine, 1998. **188**(6):1039-1046.
14. Voest, E.E., B.M. Kenyon, M.S. O'Reilly, et al., Inhibition of angiogenesis *in vivo* by interleukin 12. Journal of the National Cancer Institute, 1995. **87**(8):581-586.
15. Wels, J., R.N. Kaplan, S. Rafii, et al., Migratory neighbors and distant invaders: tumor-associated niche cells. Genes & development, 2008. **22**(5):559-574.
16. Martinez, F.O., A. Sica, A. Mantovani, et al., Macrophage activation and polarization. Frontiers in bioscience: a journal and virtual library, 2007. **13**:453-461.
17. Martinez, F.O. and S. Gordon, The M1 and M2 paradigm of macrophage activation: time for reassessment. F1000prime reports, 2014. **6**.
18. Lawrence, T. and G. Natoli, Transcriptional regulation of macrophage polarization: enabling diversity with identity. Nature reviews immunology, 2011. **11**(11):750-761.
19. Mishalian, I., R. Bayuh, L. Levy, et al., Tumor-associated neutrophils (TAN) develop pro-tumorigenic properties during tumor progression. Cancer Immunology, Immunotherapy, 2013. **62**(11):1745-1756.

20. Fridlender, Z.G., J. Sun, S. Kim, et al., Polarization of tumor-associated neutrophil phenotype by TGF-β:“N1” versus “N2” TAN. Cancer cell, 2009. **16**(3):183-194.
21. Shojaei, F., M. Singh, J.D. Thompson, et al., Role of Bv8 in neutrophil-dependent angiogenesis in a transgenic model of cancer progression. Proceedings of the National Academy of Sciences, 2008. **105**(7):2640-2645.
22. Pekarek, L.A., B.A. Starr, A.Y. Toledano, et al., Inhibition of tumor growth by elimination of granulocytes. The Journal of experimental medicine, 1995. **181**(1):435-440.
23. Tazawa, H., F. Okada, T. Kobayashi, et al., Infiltration of neutrophils is required for acquisition of metastatic phenotype of benign murine fibrosarcoma cells: implication of inflammation-associated carcinogenesis and tumor progression. The American journal of pathology, 2003. **163**(6):2221-2232.
24. Jablonska, J., S. Leschner, K. Westphal, et al., Neutrophils responsive to endogenous IFN-β regulate tumor angiogenesis and growth in a mouse tumor model. The Journal of clinical investigation, 2010. **120**(4):1151.
25. Di Carlo, E., G. Forni, P. Lollini, et al., The intriguing role of polymorphonuclear neutrophils in antitumor reactions. Blood, 2001. **97**(2):339-345.
26. de Paulis, A., N. Prevete, I. Fiorentino, et al., Expression and functions of the vascular endothelial growth factors and their receptors in human basophils. The Journal of Immunology, 2006. **177**(10):7322-7331.
27. Falkencrone, S., L.K. Poulsen, C. Bindslev‐Jensen, et al., IgE‐mediated basophil tumour necrosis factor alpha induces matrix metalloproteinase‐9 from monocytes. Allergy, 2013. **68**(5):614-620.
28. Simson, L., J.I. Ellyard, L.A. Dent, et al., Regulation of carcinogenesis by IL-5 and CCL11: a potential role for eosinophils in tumor immune surveillance. The Journal of Immunology, 2007. **178**(7):4222-4229.

29. Xie, F., L.-B. Liu, W.-Q. Shang, et al., The infiltration and functional regulation of eosinophils induced by TSLP promote the proliferation of cervical cancer cell. Cancer letters, 2015.
30. Davis, B.P. and M.E. Rothenberg, Eosinophils and cancer. Cancer immunology research, 2014. **2**(1):1-8.
31. Gatault, S., F. Legrand, M. Delbeke, et al., Involvement of eosinophils in the anti-tumor response. Cancer Immunology, Immunotherapy, 2012. **61**(9):1527-1534.
32. Carretero, R., I.M. Sektioglu, N. Garbi, et al., Eosinophils orchestrate cancer rejection by normalizing tumor vessels and enhancing infiltration of CD8+ T cells. Nature immunology, 2015. **16**(6):609-617.
33. Sugimoto, K., S. Yoshida, Y. Mashio, et al., Role of FGF10 on tumorigenesis by MS‐K. Genes to Cells, 2014. **19**(2):112-125.
34. Henan, X., N. Toyota, X. Yanjiang, et al., Enhancement of phagocytosis and cytotoxicity in macrophages by tumor-derived IL-18 stimulation. BMB Rep, 2014. **47**(5):286-91.
35. Jose, P., D. Griffiths-Johnson, P. Collins, et al., Eotaxin: a potent eosinophil chemoattractant cytokine detected in a guinea pig model of allergic airways inflammation. The Journal of experimental medicine, 1994. **179**(3):881-887.
36. Kitaura, M., T. Nakajima, T. Imai, et al., Molecular cloning of human eotaxin, an eosinophil-selective CC chemokine, and identification of a specific eosinophil eotaxin receptor, CC chemokine receptor 3. Journal of Biological Chemistry, 1996. **271**(13):7725-7730.
37. Stevenson, N.J., M.R. Addley, E.J. Ryan, et al., CCL11 blocks IL-4 and GM-CSF signaling in hematopoietic cells and hinders dendritic cell differentiation via suppressor of cytokine signaling expression. Journal of leukocyte biology, 2009. **85**(2):289-297.

38. Ponath, P.D., S. Qin, T.W. Post, et al., Molecular cloning and characterization of a human eotaxin receptor expressed selectively on eosinophils. The Journal of experimental medicine, 1996. **183**(6):2437-2448.
39. Huaux, F., M. Gharaee-Kermani, T. Liu, et al., Role of Eotaxin-1 (CCL11) and CC chemokine receptor 3 (CCR3) in bleomycin-induced lung injury and fibrosis. The American journal of pathology, 2005. **167**(6):1485-1496.
40. Levina, V., B.M. Nolen, A.M. Marrangoni, et al., Role of eotaxin-1 signaling in ovarian cancer. Clinical Cancer Research, 2009. **15**(8):2647-2656.
41. Rankin, S.M., D.M. Conroy, and T.J. Williams, Eotaxin and eosinophil recruitment: implications for human disease. Molecular medicine today, 2000. **6**(1):20-27.
42. Raschke, W., S. Baird, P. Ralph, et al., Functional macrophage cell lines transformed by Abelson leukemia virus. Cell, 1978. **15**(1):261-267.
43. Olee, T., S. Hashimoto, J. Quach, et al., IL-18 is produced by articular chondrocytes and induces proinflammatory and catabolic responses. The Journal of Immunology, 1999. **162**(2):1096-1100.
44. VanderBrink, B.A., K. Hile, H. Asanuma, et al., 283 IL-18 STIMULATES A POSITIVE FEEDBACK LOOP THROUGH THE IL-18 RECEPTOR DURING RENAL OBSTRUCTION. The Journal of Urology, 2010. **183**(4):e112.
45. Graells, J., A. Vinyals, A. Figueras, et al., Overproduction of VEGF165 concomitantly expressed with its receptors promotes growth and survival of melanoma cells through MAPK and PI3K signaling. Journal of Investigative Dermatology, 2004. **123**(6):1151-1161.
46. Sica, A., P. Allavena, and A. Mantovani, Cancer related inflammation: the macrophage connection. Cancer letters, 2008. **267**(2):204-215.
47. Sica, A., T. Schioppa, A. Mantovani, et al., Tumour-associated macrophages are a distinct M2 polarised population promoting tumour progression: potential targets of anti-cancer therapy. European journal of cancer, 2006. **42**(6):717-727.

48. Allavena, P., A. Sica, G. Solinas, et al., The inflammatory micro-environment in tumor progression: the role of tumor-associated macrophages. Critical reviews in oncology/hematology, 2008. **66**(1):1-9.
49. Mantovani, A., S. Sozzani, M. Locati, et al., Macrophage polarization: tumor-associated macrophages as a paradigm for polarized M2 mononuclear phagocytes. Trends in immunology, 2002. **23**(11):549-555.
50. Biswas, S.K. and A. Mantovani, Macrophage plasticity and interaction with lymphocyte subsets: cancer as a paradigm. Nature immunology, 2010. **11**(10):889-896.
51. Okamura, H., H. Tsutsui, T. Komatsu, et al., Cloning of a new cytokine that induces IFN-γ production by T cells. Nature, 1995. **378**(6552):88-91.
52. Xie, Q.-W., H.J. Cho, J. Calaycay, et al., Cloning and characterization of inducible nitric oxide synthase from mouse macrophages. Science, 1992. **256**(5054):225-228.
53. Ryan, A., A. Colleran, A. O'Gorman, et al., Targeting colon cancer cell NF-κB promotes an anti-tumour M1-like macrophage phenotype and inhibits peritoneal metastasis. Oncogene, 2015. **34**(12):1563-1574.
54. Hatzi, E., C. Murphy, A. Zoephel, et al., N-myc oncogene overexpression down-regulates IL-6; evidence that IL-6 inhibits angiogenesis and suppresses neuroblastoma tumor growth. Oncogene, 2002. **21**(22):3552-3561.
55. Sharma, J., A. Al-Omran, and S. Parvathy, Role of nitric oxide in inflammatory diseases. Inflammopharmacology, 2007. **15**(6):252-259.
56. Dealtry, G., M. Naylor, W. Fiers, et al., The effect of recombinant human tumour necrosis factor on growth and macromolecular synthesis of human epithelial cells. Experimental cell research, 1987. **170**(2):428-438.

57. Motoo, Y., N. Hill, M. Mahmoudi, et al., Antitumor effect of human necrosis factor on human hepatoma cells PLC/PRF/5. The Japanese journal of experimental medicine, 1986. **56**(4):151-154.
58. Haranaka, K., N. Satomi, and A. Sakurai, Antitumor activity of murine tumor necrosis factor (TNF) against transplanted murine tumors and heterotransplanted human tumors in nude mice. International Journal of Cancer, 1984. **34**(2):263-267.
59. Li, D., C. Beisswenger, C. Herr, et al., Expression of the antimicrobial peptide cathelicidin in myeloid cells is required for lung tumor growth. Oncogene, 2014. **33**(21):2709-2716.
60. Lungarella, G., R. Menegazzi, C. Gardi, et al., Identification of elastase in human eosinophils: immunolocalization, isolation, and partial characterization. Archives of biochemistry and biophysics, 1992. **292**(1):128-135.
61. Foekens, J.A., C. Ries, M.P. Look, et al., The prognostic value of polymorphonuclear leukocyte elastase in patients with primary breast cancer. Cancer research, 2003. **63**(2):337-341.
62. To, K.K. and L.E. Huang, Suppression of hypoxia-inducible factor 1α (HIF-1α) transcriptional activity by the HIF prolyl hydroxylase EGLN1. Journal of Biological Chemistry, 2005. **280**(45):38102-38107.
63. Erez, N., M. Milyavsky, R. Eilam, et al., Expression of prolyl-hydroxylase-1 (PHD1/EGLN2) suppresses hypoxia inducible factor-1α activation and inhibits tumor growth. Cancer research, 2003. **63**(24):8777-8783.
64. Epstein, A.C., J.M. Gleadle, L.A. McNeill, et al., C. elegans EGL-9 and mammalian homologs define a family of dioxygenases that regulate HIF by prolyl hydroxylation. Cell, 2001. **107**(1):43-54.

65. Lamkhioued, B., S.G. Abdelilah, Q. Hamid, et al., The CCR3 receptor is involved in eosinophil differentiation and is up-regulated by Th2 cytokines in CD34+ progenitor cells. The Journal of Immunology, 2003. **170**(1):537-547.
66. Voehringer, D., N. Van Rooijen, and R.M. Locksley, Eosinophils develop in distinct stages and are recruited to peripheral sites by alternatively activated macrophages. Journal of leukocyte biology, 2007. **81**(6):1434-1444.
67. Bochner, B.S., Siglec‐8 on human eosinophils and mast cells, and Siglec‐F on murine eosinophils, are functionally related inhibitory receptors. Clinical & Experimental Allergy, 2009. **39**(3):317-324.
68. Sonoda, Y., N. Arai, and M. Ogawa, Humoral regulation of eosinophilopoiesis *in vitro*: analysis of the targets of interleukin-3, granulocyte/macrophage colony-stimulating factor (GM-CSF), and interleukin-5. Leukemia, 1989. **3**(1):14-18.
69. Lopez, A.F., C.G. Begley, D.J. Williamson, et al., Murine eosinophil differentiation factor. An eosinophil-specific colony-stimulating factor with activity for human cells. The Journal of experimental medicine, 1986. **163**(5):1085-1099.
70. Bettigole, S.E., R. Lis, S. Adoro, et al., The transcription factor XBP1 is selectively required for eosinophil differentiation. Nature immunology, 2015. **16**(8):829-837.
71. Salcedo, R., H.A. Young, M.L. Ponce, et al., Eotaxin (CCL11) induces *in vivo* angiogenic responses by human CCR3+ endothelial cells. The Journal of Immunology, 2001. **166**(12):7571-7578.
72. Cormier, S.A., A.G. Taranova, C. Bedient, et al., Pivotal Advance: eosinophil infiltration of solid tumors is an early and persistent inflammatory host response. Journal of leukocyte biology, 2006. **79**(6):1131-1139.
73. Samoszuk, M., T. Deng, M.J. Hamamura, et al., Increased blood clotting, microvascular density, and inflammation in eotaxin-secreting tumors implanted into mice. The American journal of pathology, 2004. **165**(2):449-456.

74. Ran, F.A., P.D. Hsu, J. Wright, et al., Genome engineering using the CRISPR-Cas9 system. Nature protocols, 2013. **8**(11):2281-2308.
75. Epstein, F.H. and M.E. Rothenberg, Eosinophilia. New England Journal of Medicine, 1998. **338**(22):1592-1600.

Supplemental Table1. List of PCR primers

Gene	Accession	Forward primer (5'-)	Reverse primer (5'-)	Product size (bp)	Annealing temp (°C)
il-18 (For vector construction)	NM_008360	ttgctagcccatgaactttggccgactt	cacctcgagctaactttgatgtaagttagtg	494	60
il-18	NM_008360	atcaaagtgccagtgaaccc	tcaggtggatccatttcctc	160	60
il-18 r1	NM_008365	gcattctcattgttaaaagtgcc	caaggtgtgatcatgaaaagtga	221	60
il-18 rap	NM_010553	acatattctgcaaggggtgc	tatgcagcatgccttcactc	241	60
vegf-a	NM_001025250	gaccctggctttactgctgta	gtgaggtttgatccgcatgat	303	58
nos2	NM_010927	tcaccttcgagggcagccga	tccgtggcaaagcgagccag	286	60
il-6	NM_031168	gcacttgcagaaaacaatctg	tctgaaggactctggctttgt	187	54
il-10	NM_010548	acatactgctaaccgactcct	actcttcacctgctccact	245	63
cd86	NM_019388	aggaacaactggactctacga	ttcttaggtttcgggtgaccttg	236	60
mrc1	NM_008625	catctcagttcagacggcaa	ccttcctactgctccacaat	299	59

ccl11 (For vector construction)	NM_011330	cgtcagatccgctagcaccATGcacccaggctc	gaagcttgagctcgattatggttttggagtttggag	256	60
ccl11	NM_011330	cctgctgctttatcatgacc	gagtttttggtccaggtgct	185	60
tnf-α	NM_001278601	ggttctgtccctttcactca	agccataatccccttttctaa	892	60
camp	NM_009921	gacaccaatctctaccgtctcc	tgccacatacagtctccttcac	109	53
cela2a	NM_007919	tggcaccattctcccgag	catagtccacaaccagcaggc	116	54
egln1	NM_053207	gataacccaaatggagatggaa	gttcaaccctcacacctttctc	298	50
egln2	NM_053208	gtacgtgaggcatgttgacaat	ttggcatcaaaataccagacag	255	50
egln3	NM_028133	caggaaatgggacaggttatgt	tcttcagcatcgaagtaccaga	274	50
siglec-f	NM_001271019	tatattcagcggctctccag	ggcacagaacagagcagttt	297	60
ccr3	NM_009914	aaggacttagcaaaattcacca	acaccagggagtacagtgga	179	52
cd80	NM_009855	ctgaagaccgaatctactggcaa	ccttttagtgtctgcagatgggt	296	60
ym1	NM_009892	ttgtgggatttccagcatatggg	acggcacctcctaaattgttgtc	293	53
f4/80	NM_010130	gccacctgcactgacaccaca	agctgcacttggctctcccca	190	60
β-actin	NM_007393	cagggtgtgatggtgggaatggg	caggatggcgtgagggagagca	408	60

Supplemental table 2. Comparisons of Xbp1 expression in MS-K and NFSA cells

Gene	Accession No.	Signal		Log2 ratio
		MS-K	NFSA	(MS-K/NFSA)
X-box binding protein1 (Xbp1)	NM_013842	62092.6	30135.5	1.04

The gene expression was analyzed by DNA microarray. Table represents part of the data. Signal indicates the expression levels of each gene in MS-K or NFSA cells. The log2 ratio means the relative expression of each gene in MS-K against in NFSA cells.

Acknowledgements

At the very beginning, I would like to present my sincere gratitude to my supervisor, Dr. Sugimoto, a responsible, respectable and generous scholar, for his consistent and illuminating instruction during my doctoral program.

Meanwhile, I should show my appreciation to Dr.Touma, for her helpful suggestion and valuable guidance on the progress of this research.

I shall extend my thanks to the members in Sugimoto Lab, Dr. Xu, Mr. Tian, Mr. Kurosawa, and Ms. Matsui, for their kind help and providing a pleasant atmosphere in the lab. And specific thanks to Dr. Huang for his help of the data analysis.

I would also like to thank all my professors and teachers in Graduate School of Science and Technology who have helped me to develop the fundamental and essential academic competence.

Last but not least, I'd like to thank my beloved parents and my family for their continuous encouragement and support. And I shall thank to my girlfriend Pang Meiling for her selfless help and kind inspiration for me to overcome the difficulties in the studies and daily life.

By four and a half years efforts and progress, this is not just an end, but a fresh beginning for me to explore more and learn more on this road.